Electronic Supplementary Information

for

Physical properties and cytotoxicity of the Cu(II) and Zn(II) complexes with TMS-substituted indolo[2,3-*c*]quinoline-derived Schiff base

Christopher Wittmann,[a] Iuliana Besleaga,[a] Soheil Mahmoudi,[a,b] Oleg Palamarciuc,[c,d] Mihaela Balan-Porcarasu,[e] Mihaela Dascalu,[c] Sergiu Shova,[c] Maria Cazacu,[c] Mónika Kiricsi,[f] Nóra Igaz,[f] Orsolya Dömötör,[g] Eva A. Enyedy,[g,*] Dana Dvoranová,[h] Peter Rapta,[h,*] Vladimir B. Arion[a,c,*]

[a]*University of Vienna, Institute of Inorganic Chemistry, Währinger Strasse 42, 1090 Vienna, Austria*

[b]*University of Vienna, Vienna Doctoral School in Chemistry (DoSChem), Währinger Strasse 42, 1090 Vienna, Austria*

[c]*Inorganic Polymers Department, "Petru Poni" Institute of Macromolecular Chemistry, Aleea Gr. Ghica Voda 41 A, Iasi 700487, Romania*

[d]*Physics of Semiconductors and Devices Laboratory, Faculty of Physics and Engineering and Institute of Applied Physics, Moldova State University, MD-2009 Chişinău, Republic of Moldova*

[e]*NMR Laboratory, "Petru Poni" Institute of Macromolecular Chemistry, Aleea Gr. Ghica Voda 41 A, Iasi 700487, Romania*

[f]*Department of Biochemistry and Molecular Biology, University of Szeged, Közép fasor 52, H-6726 Szeged, Hungary*

[g]*Department of Molecular and Analytical Chemistry, Interdisciplinary Excellence Centre, University of Szeged, Dóm tér 7-8, H-6720 Szeged, Hungary*

[h]*Institute of Physical Chemistry and Chemical Physics, Faculty of Chemical and Food Technology, Slovak University of Technology in Bratislava, SK-81237 Bratislava, Slovakia*

Table of Contents

NMR Numbering Scheme

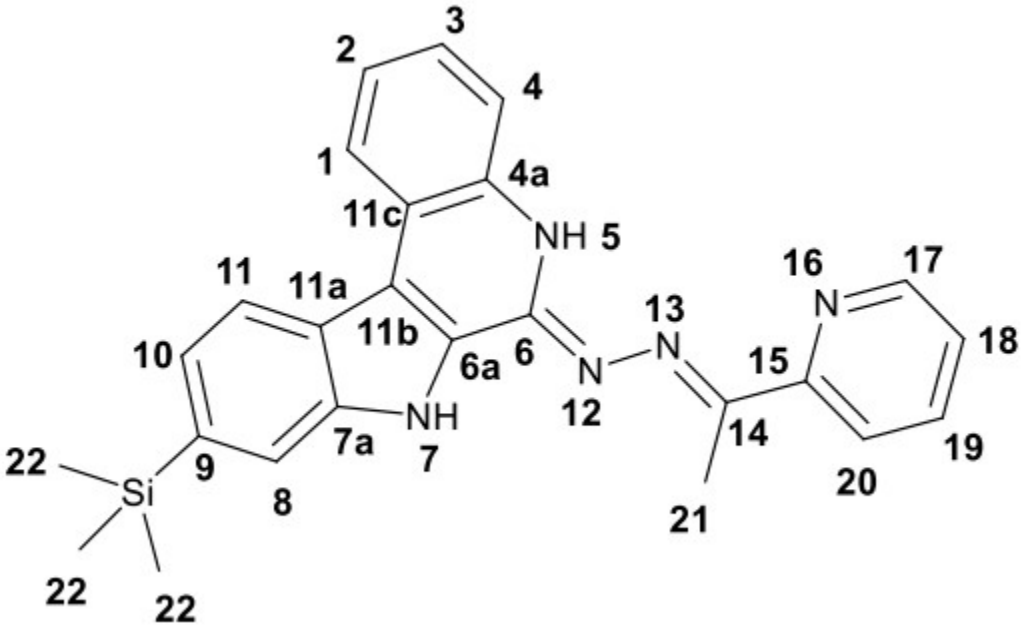

Figure S1. NMR atom numbering scheme for **HL^{TMS}**.

NMR data for organic compounds

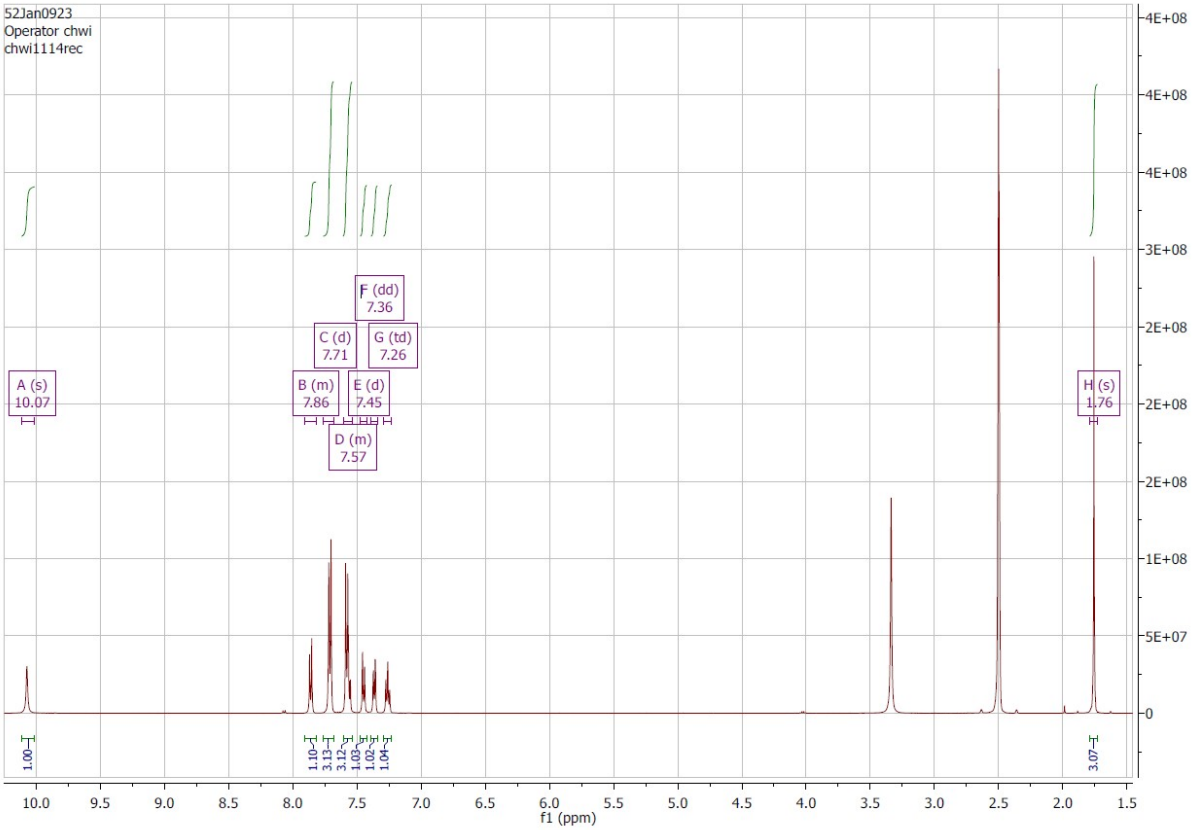

Figure S2. ^{1}H NMR spectrum of species **A** in DMSO-d_6.

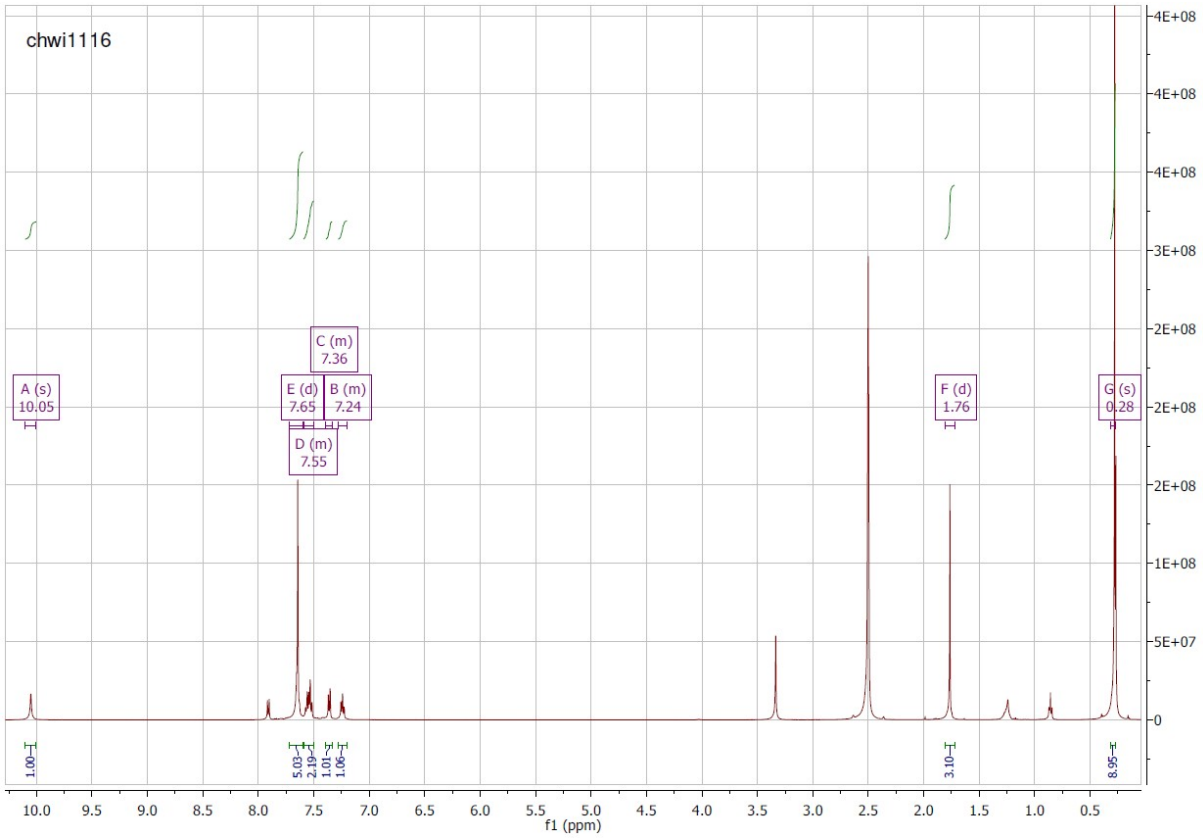

Figure S3. ^{1}H NMR spectrum of species **B** in DMSO-d_6.

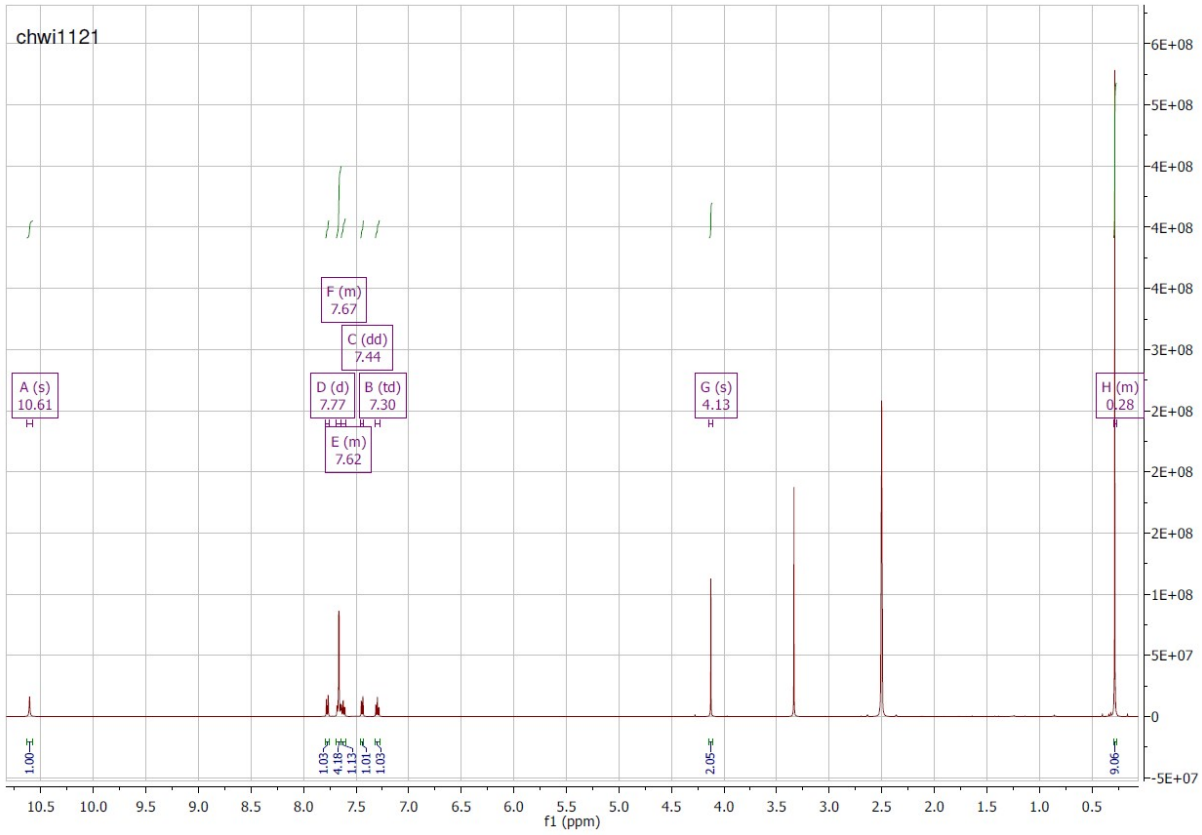

Figure S4. ^{1}H NMR spectrum of species **D** in DMSO-d_6.

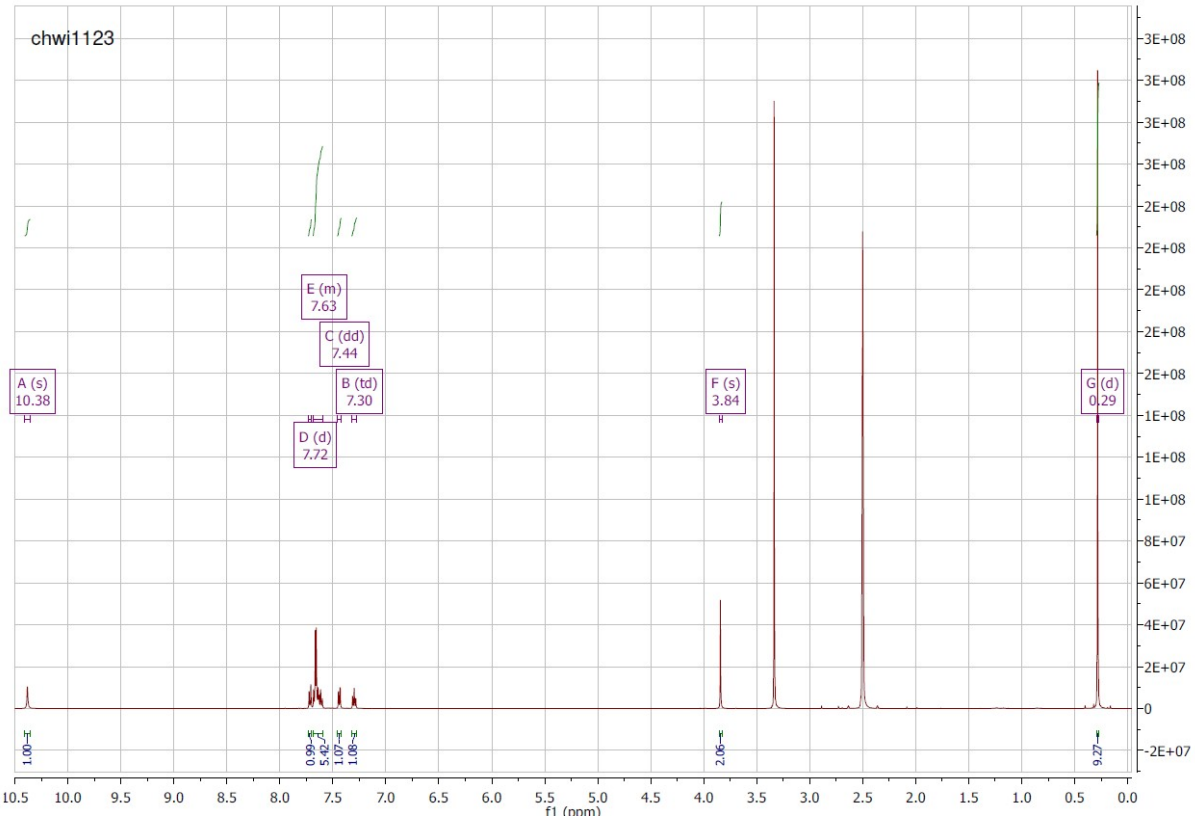

Figure S5. ^{1}H NMR spectrum of species **E** in DMSO-d_6.

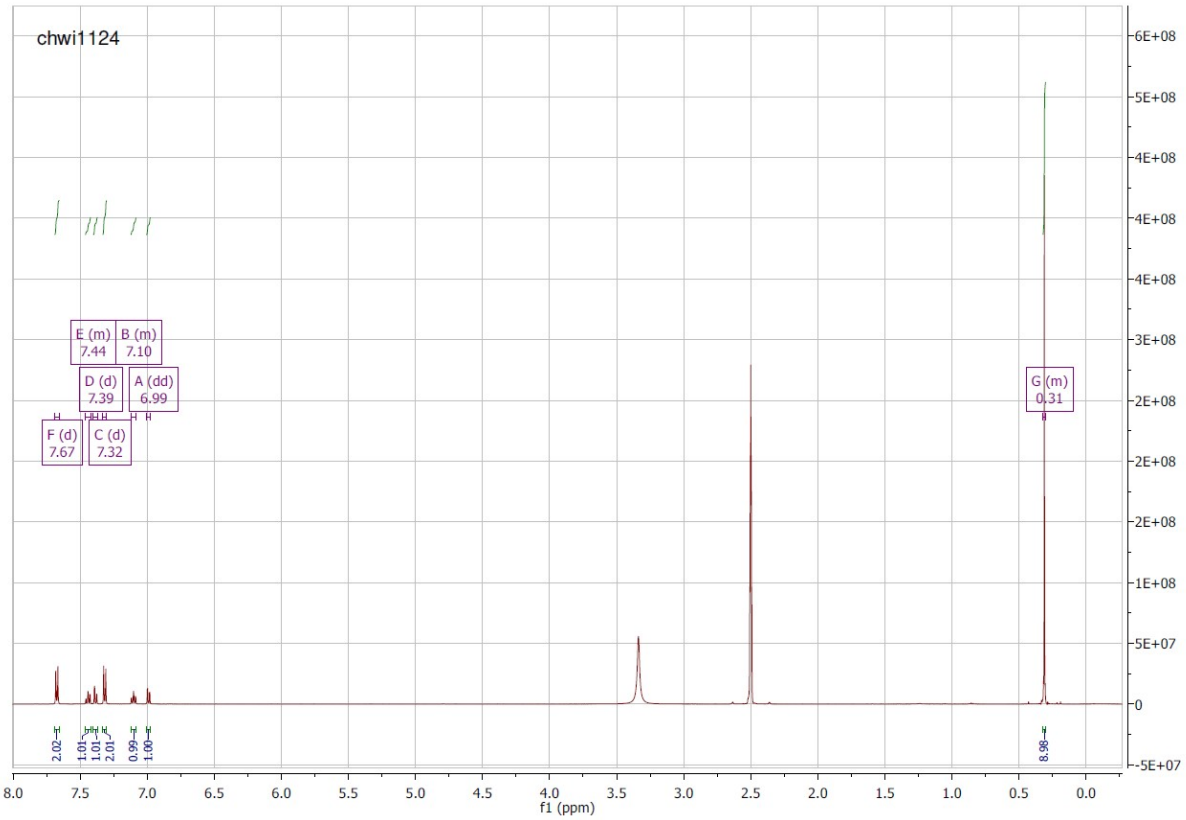

Figure S6. ^{1}H NMR spectrum of species **F** in DMSO-d_6.

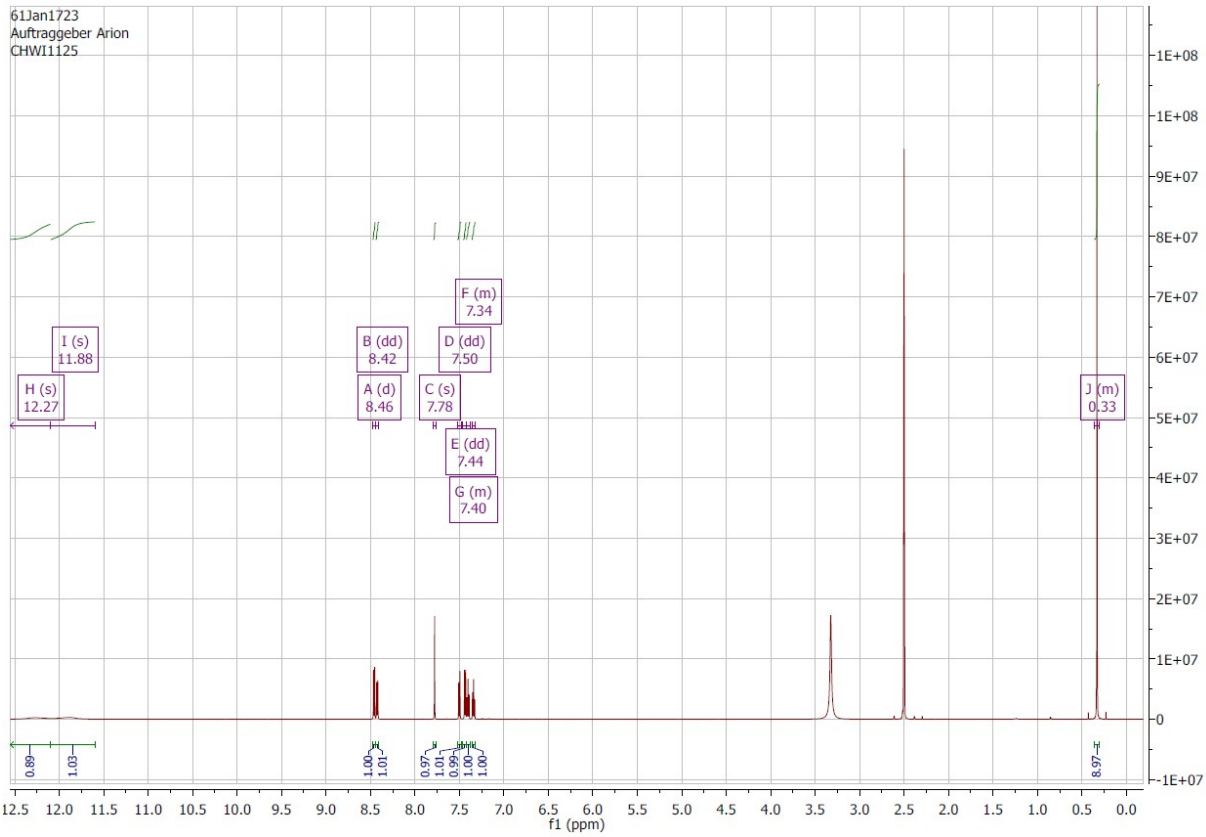

Figure S7. ^{1}H NMR spectrum of species **G** in DMSO-d_6.

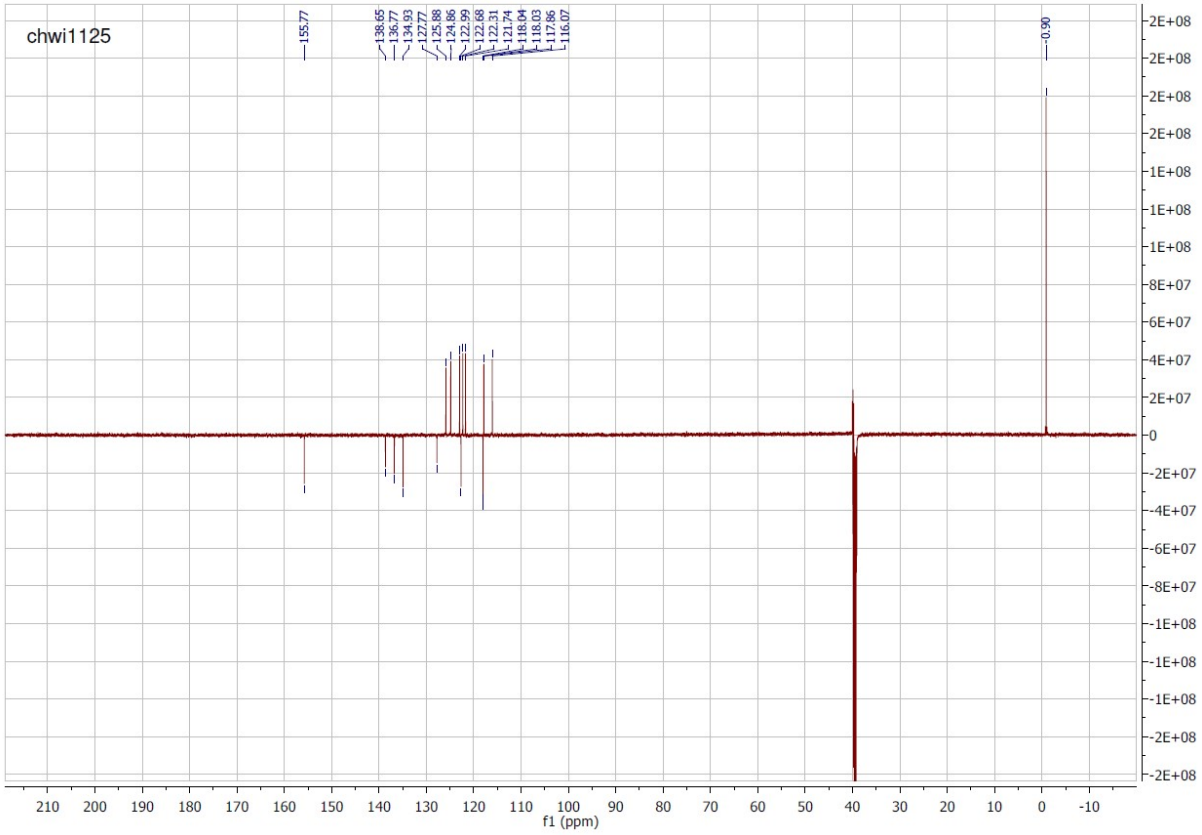

Figure S8. ^{13}C NMR spectrum of species **G** in DMSO-d_6.

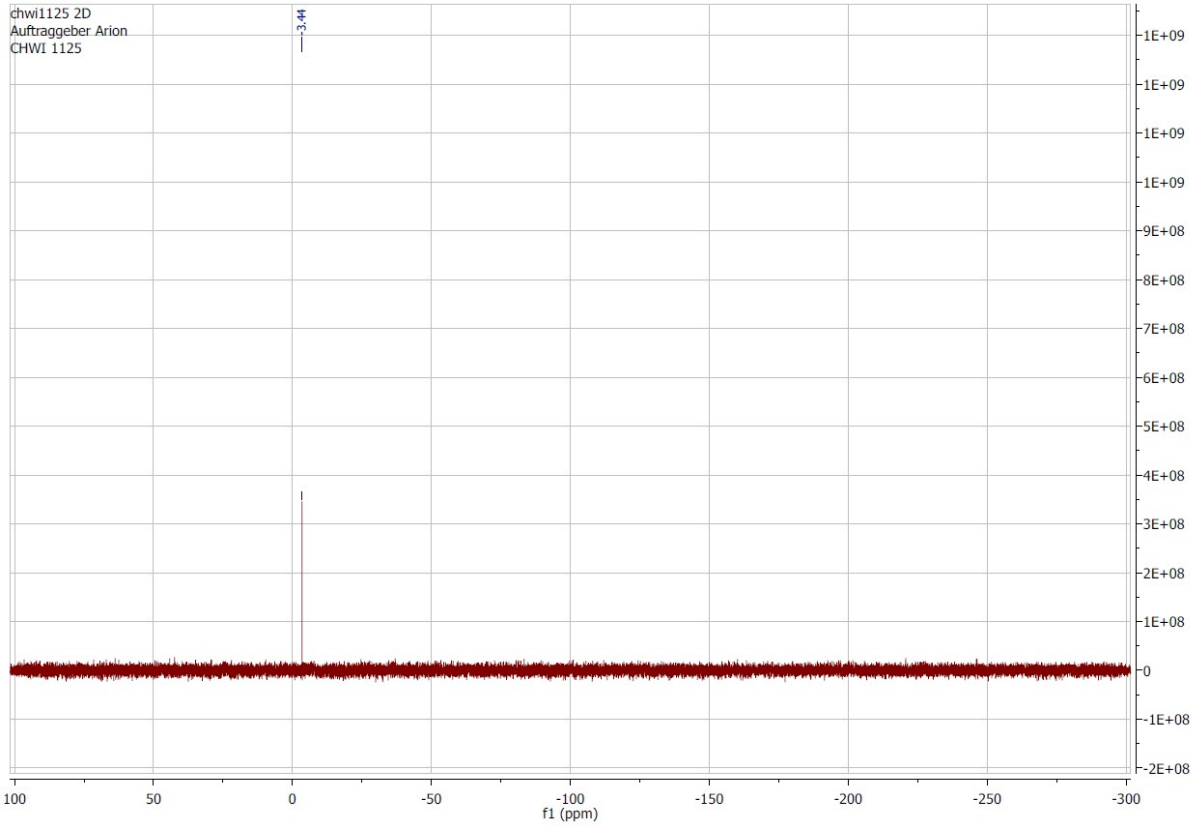

Figure S9. ^{29}Si NMR spectrum of species **G** in DMSO-d_6.

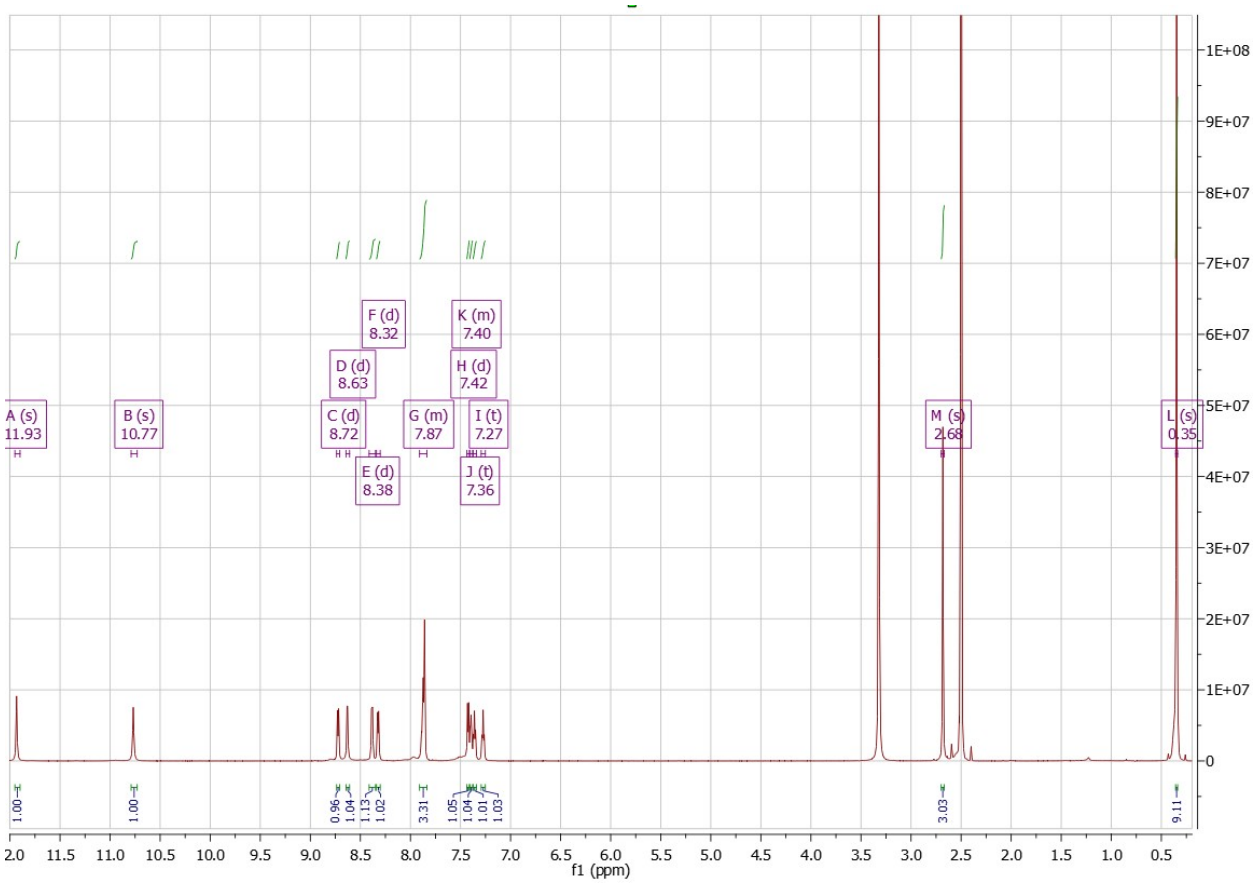

Figure S10. ^{1}H NMR spectrum of **HL^{TMS}** in DMSO-d_6.

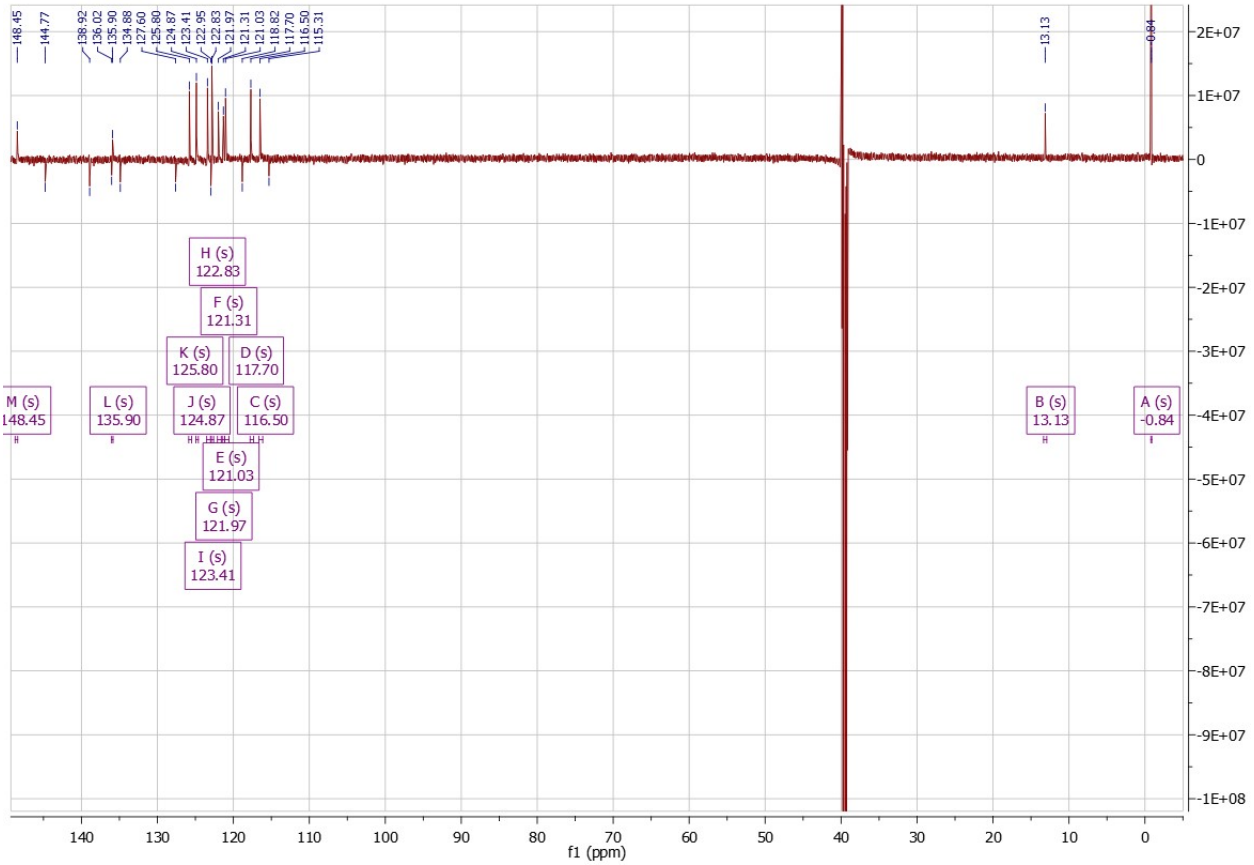

Figure S11. ^{13}C NMR spectrum of **HL^{TMS}** in DMSO-d_6.

ESI-MS for organic compounds

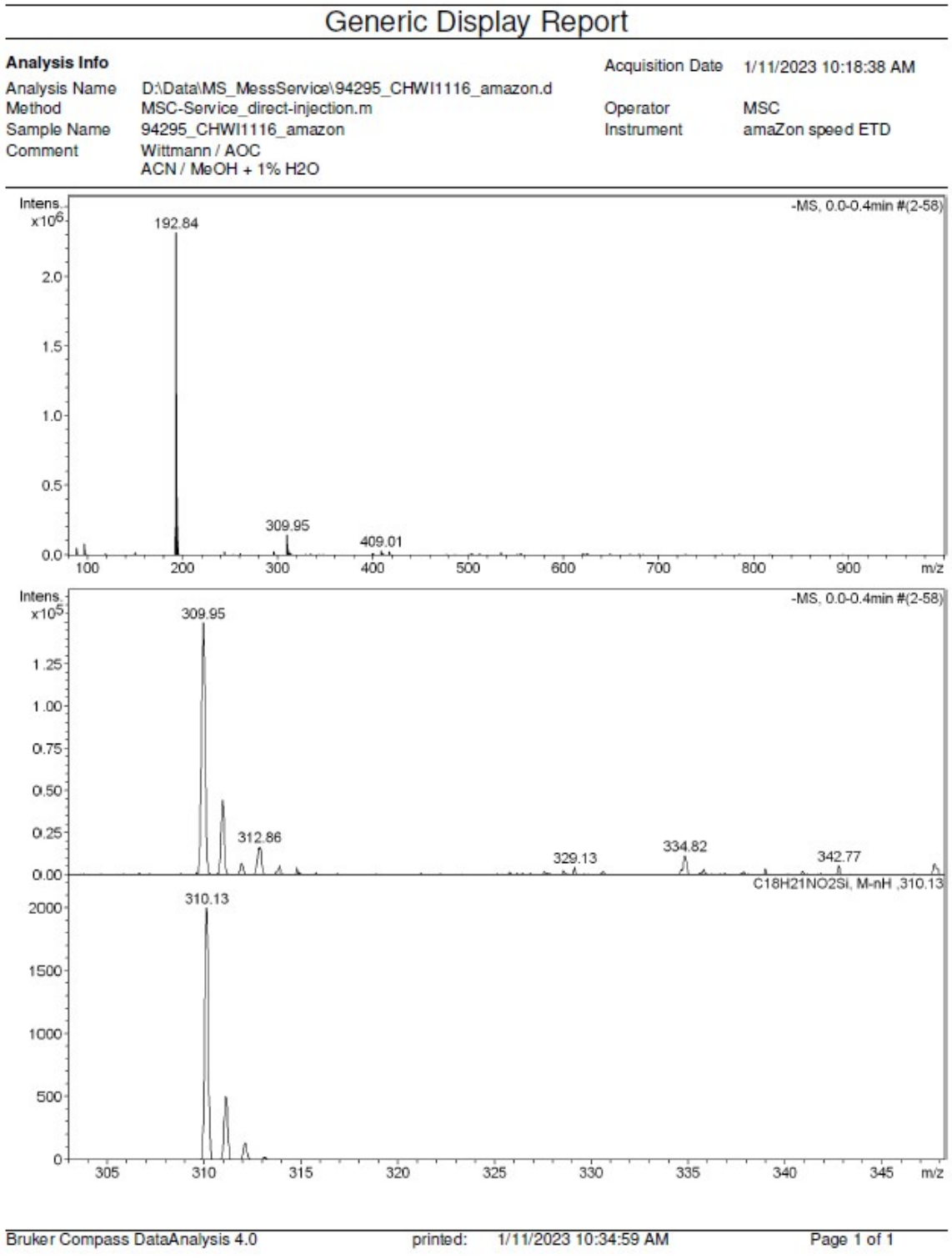

Figure S12. ESI(+) mass spectrum of **B**.

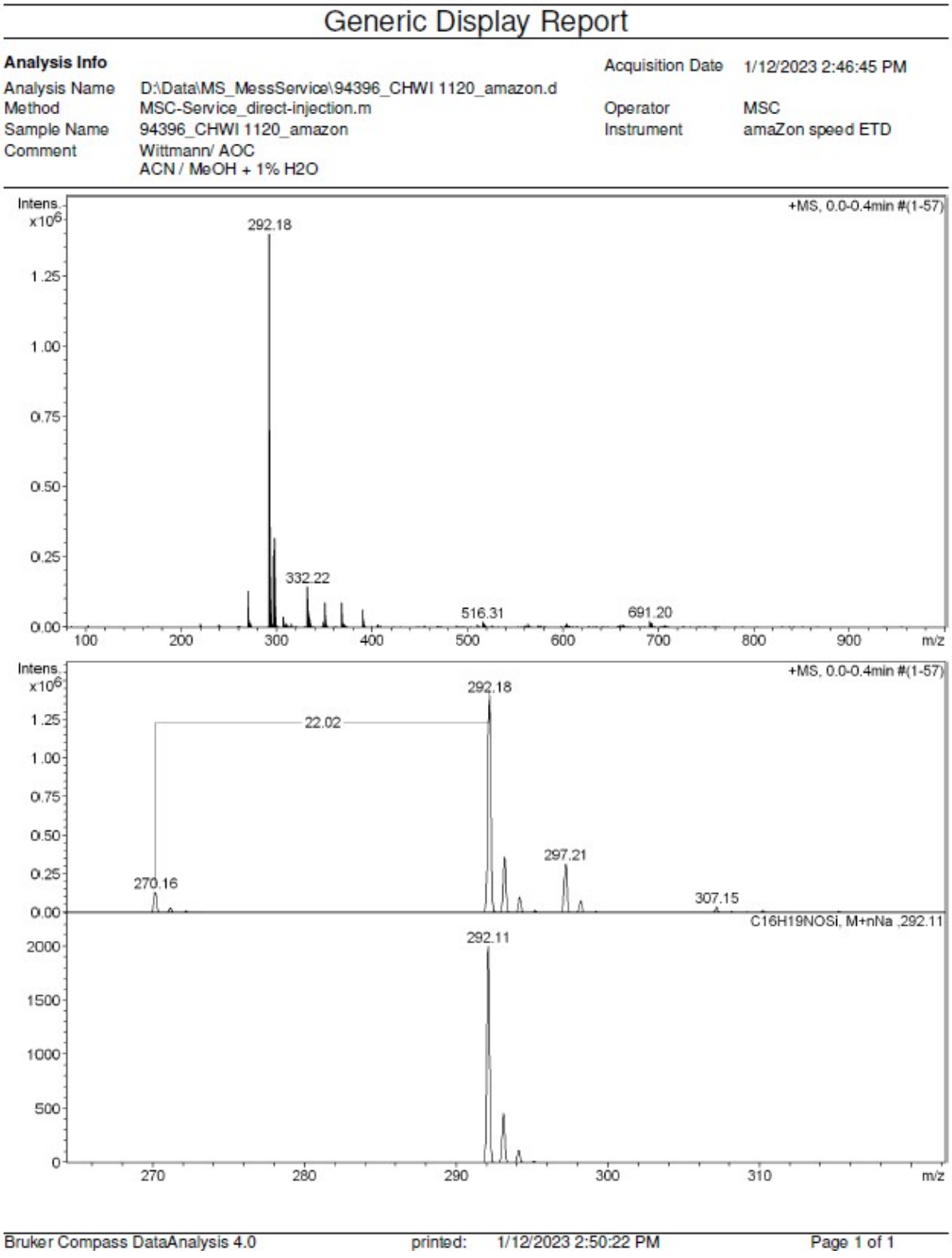

Figure S13. ESI(+) mass spectrum of **C**.

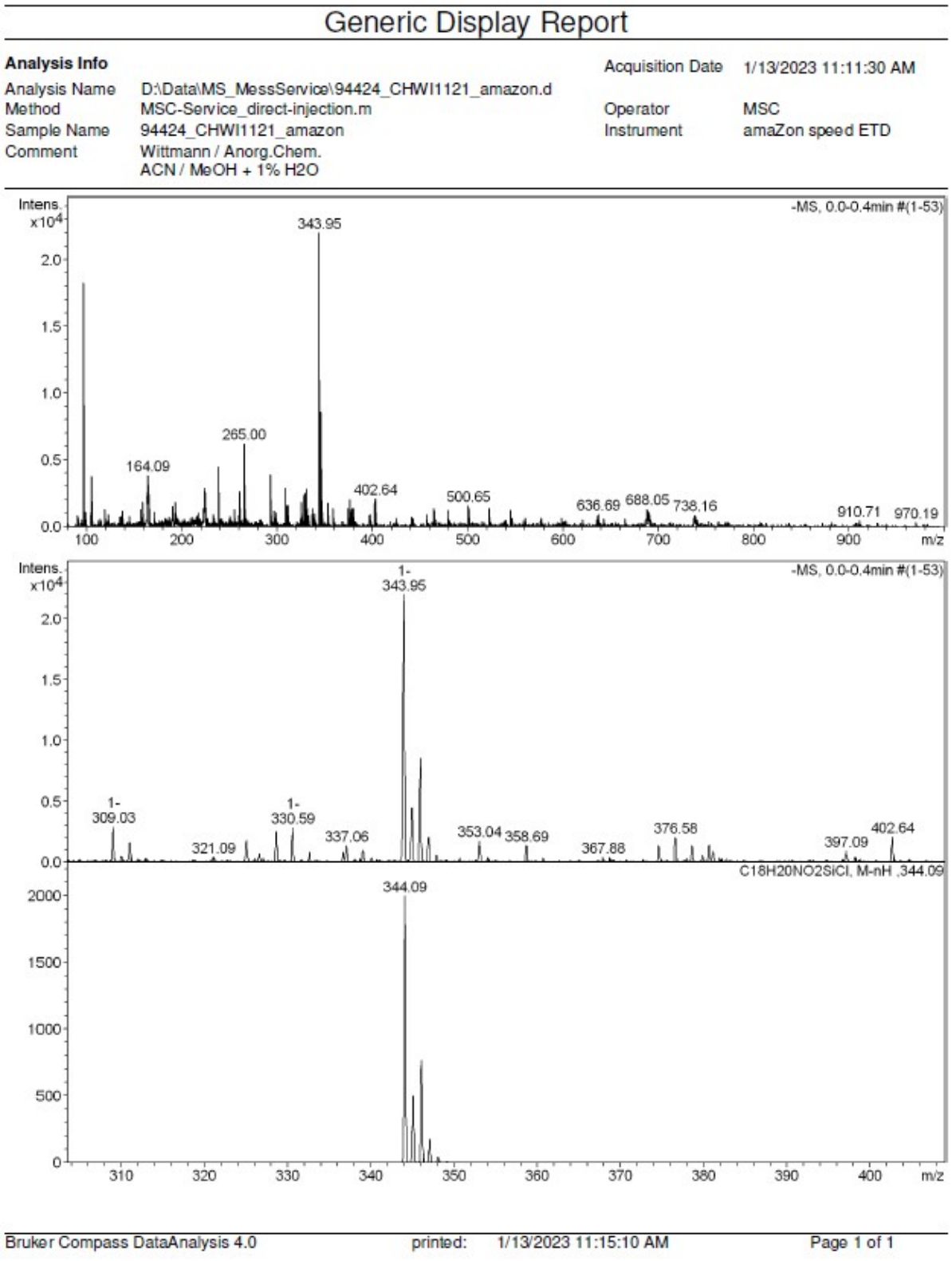

Figure S14. ESI(+) mass spectrum of **D**.

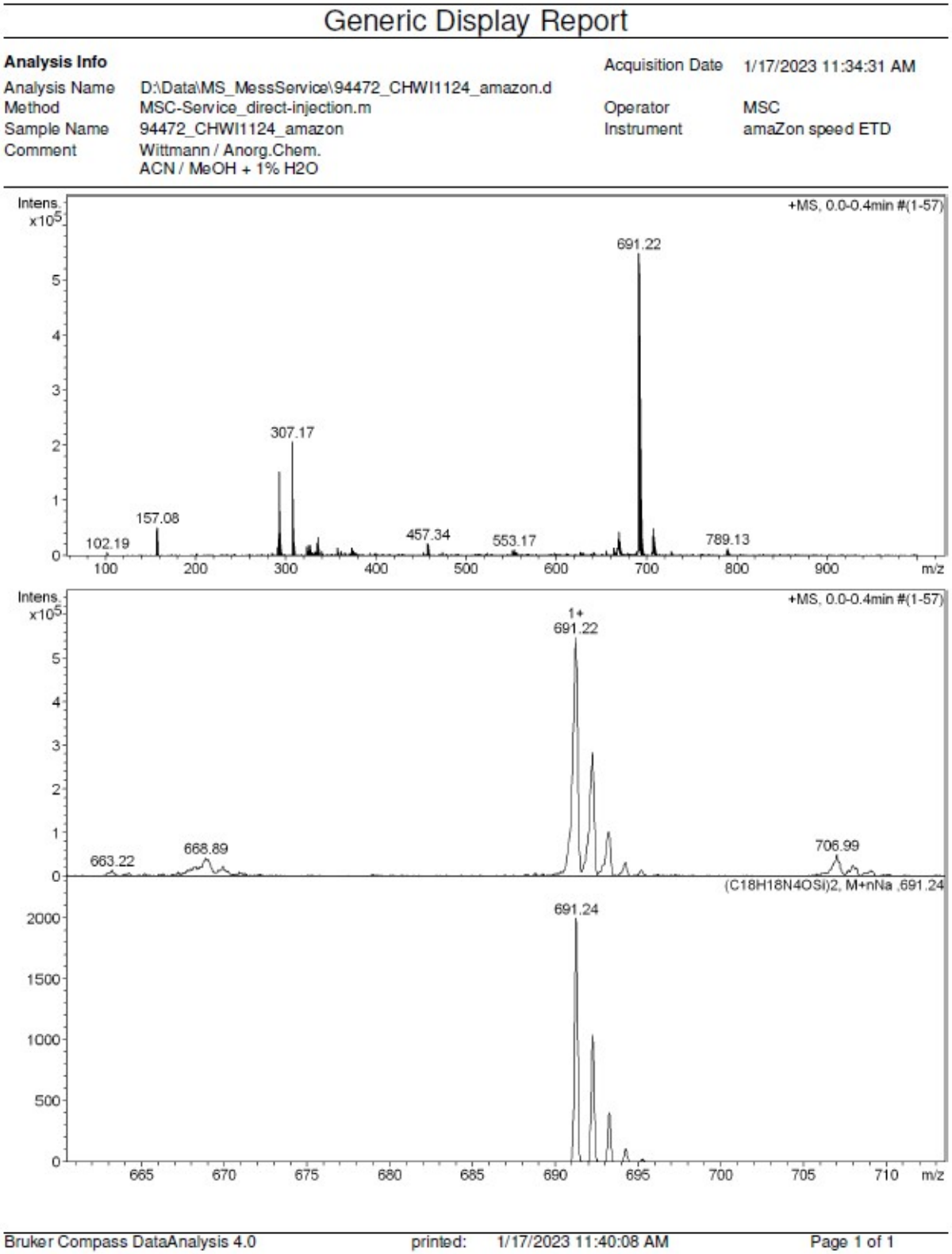

Figure S15. ESI(+) mass spectrum of **F**.

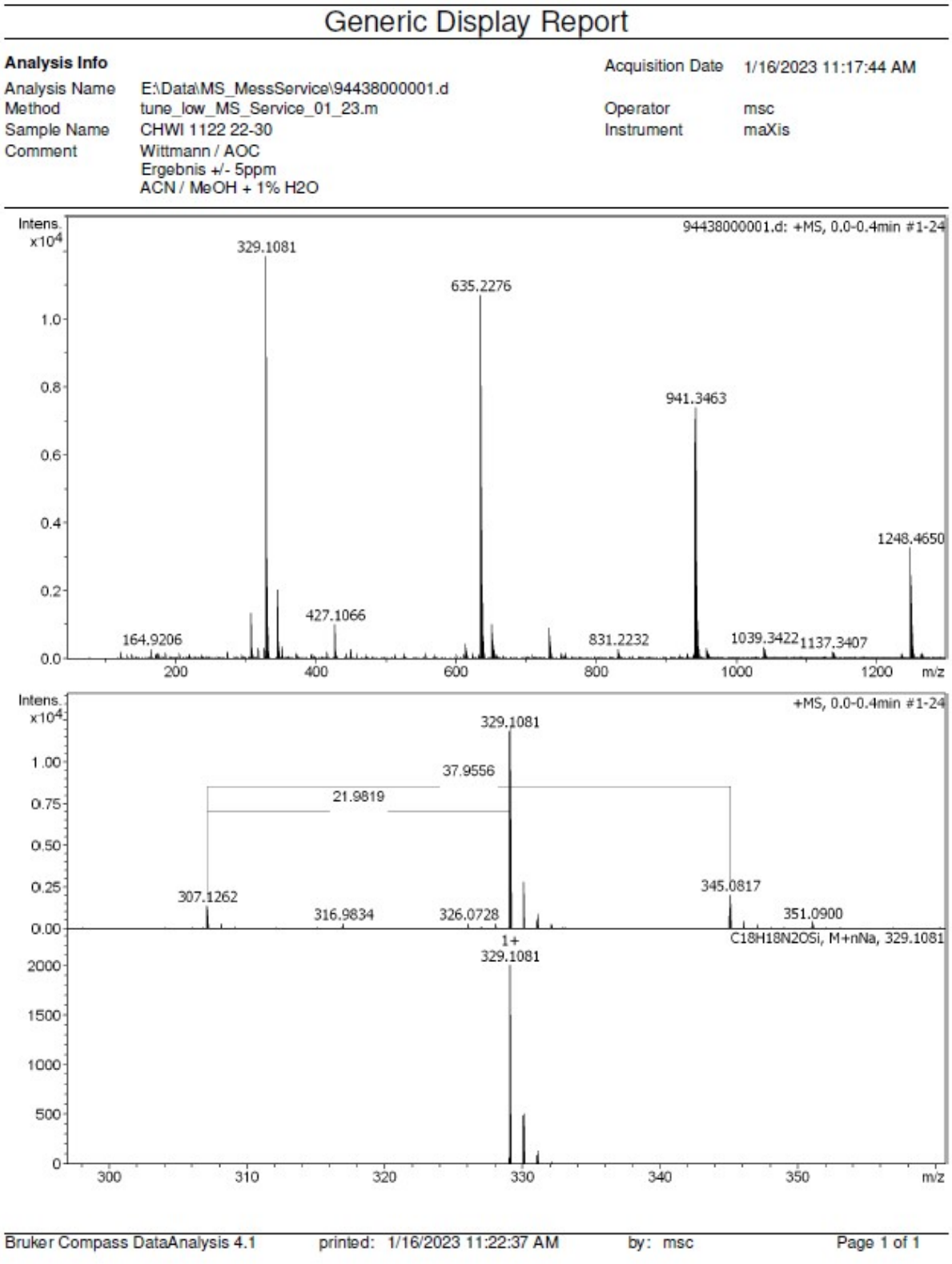

Figure S16. ESI(+) mass spectrum of **G**.

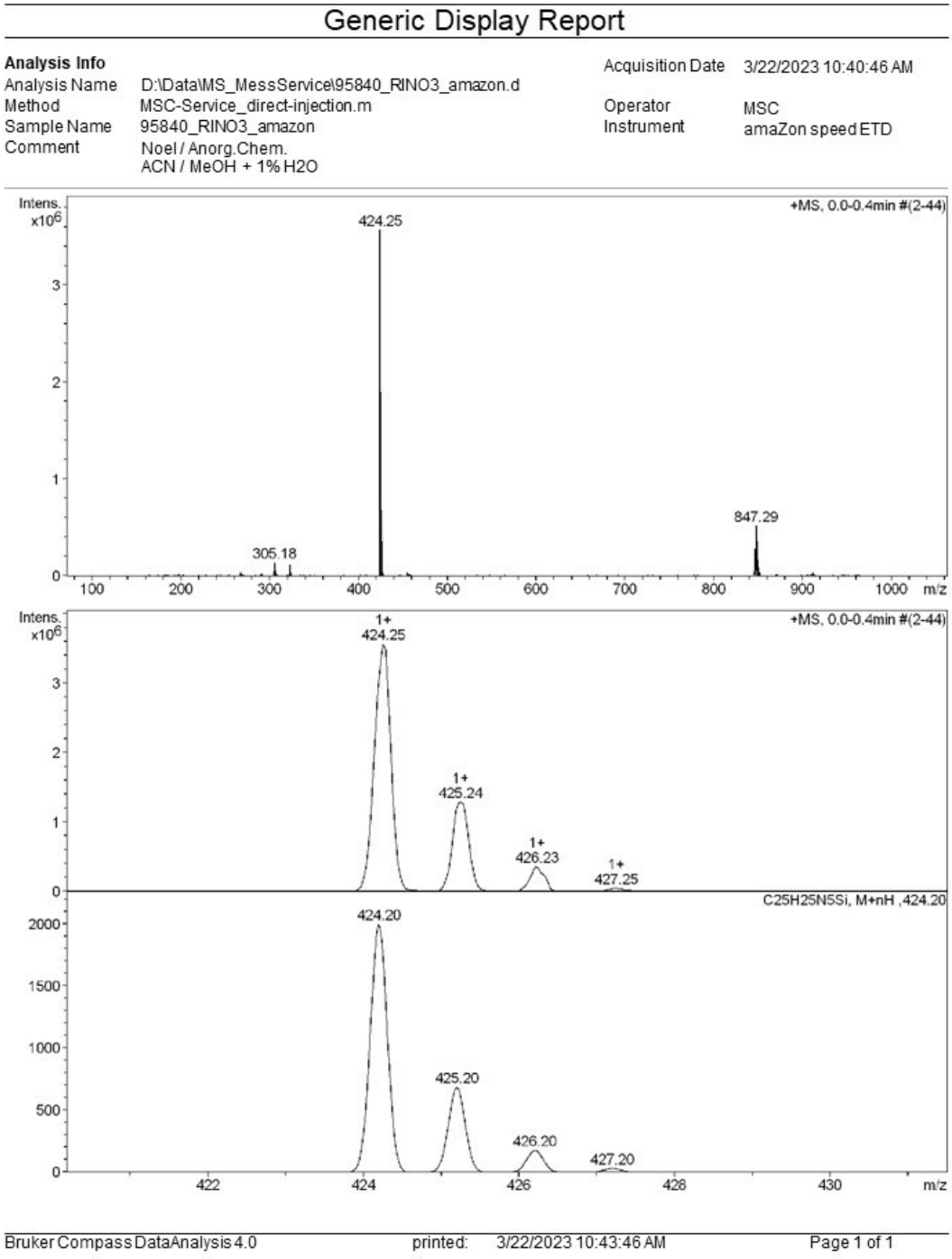

Figure S17. ESI(+) mass spectrum of **HL^{TMS}**.

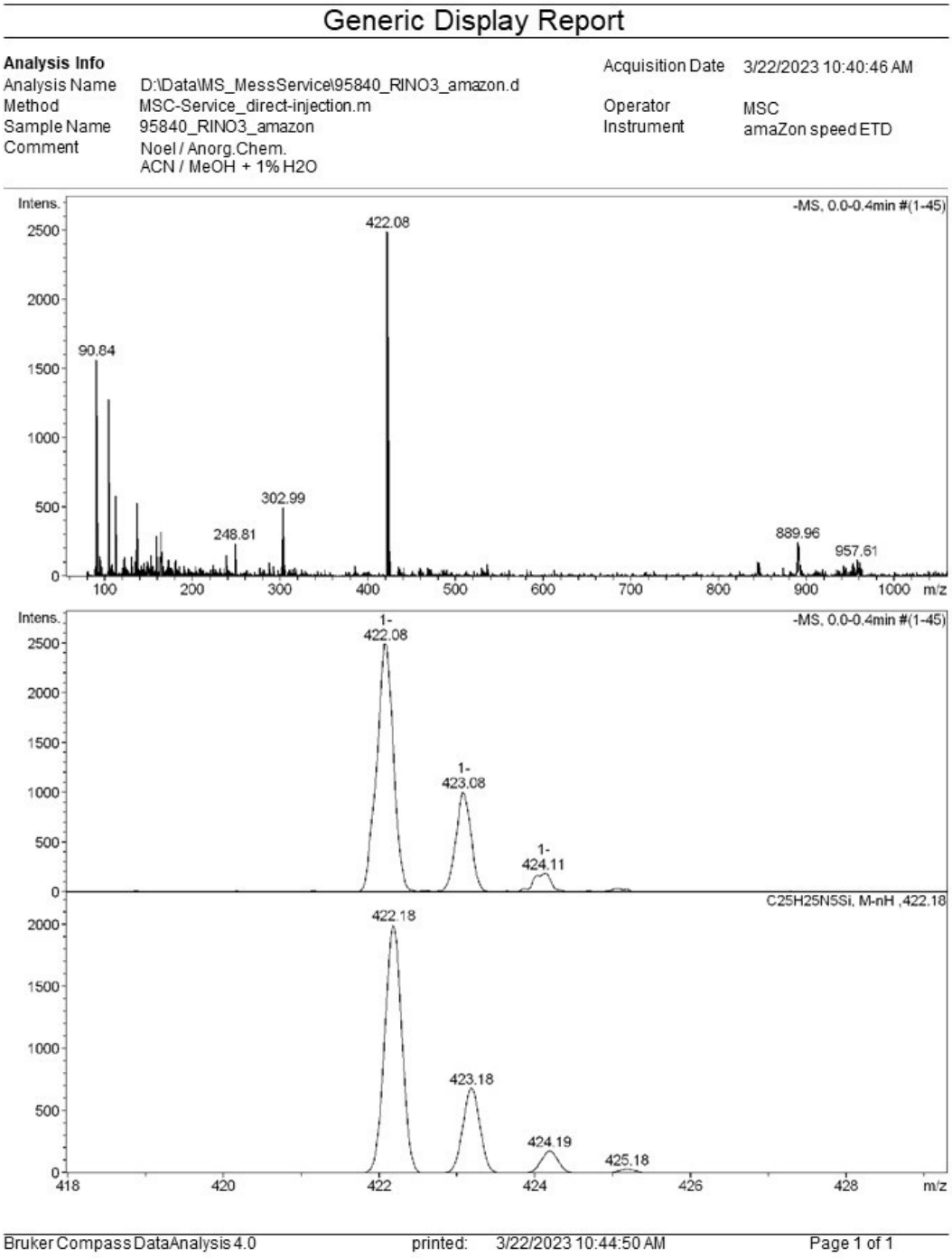

Figure S18. ESI(−) mass spectrum of **HL^{TMS}**.

NMR spectra of Zn(II) complex 2

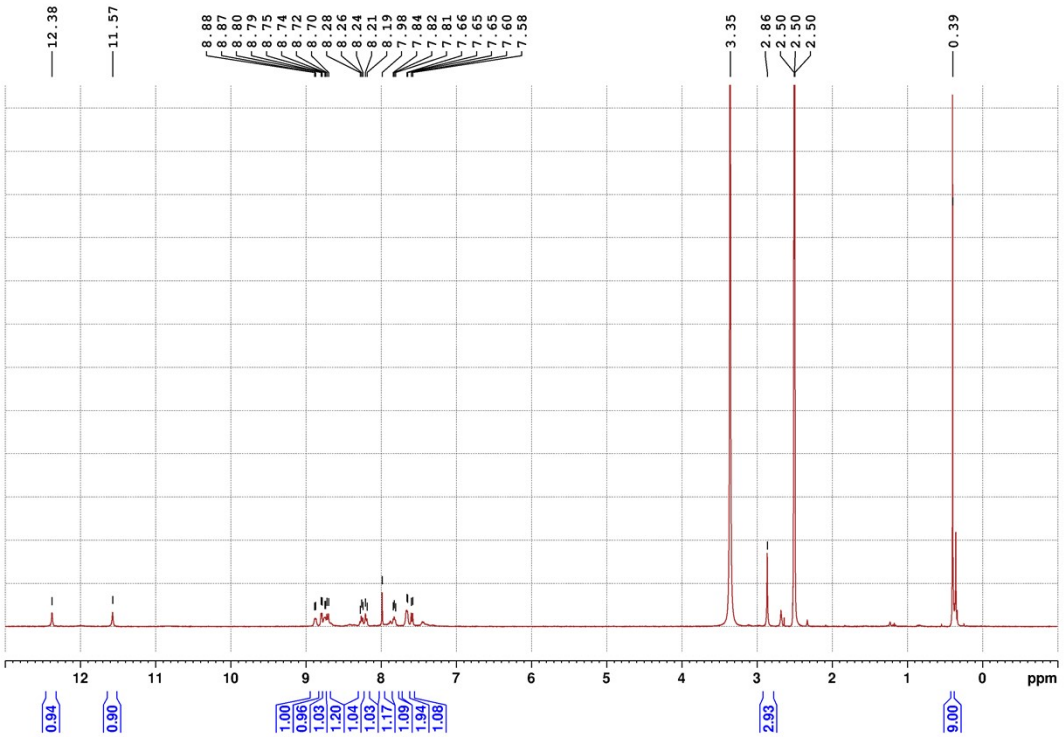

Figure S19. ^{1}H NMR spectrum of **2** in DMSO-d_6.

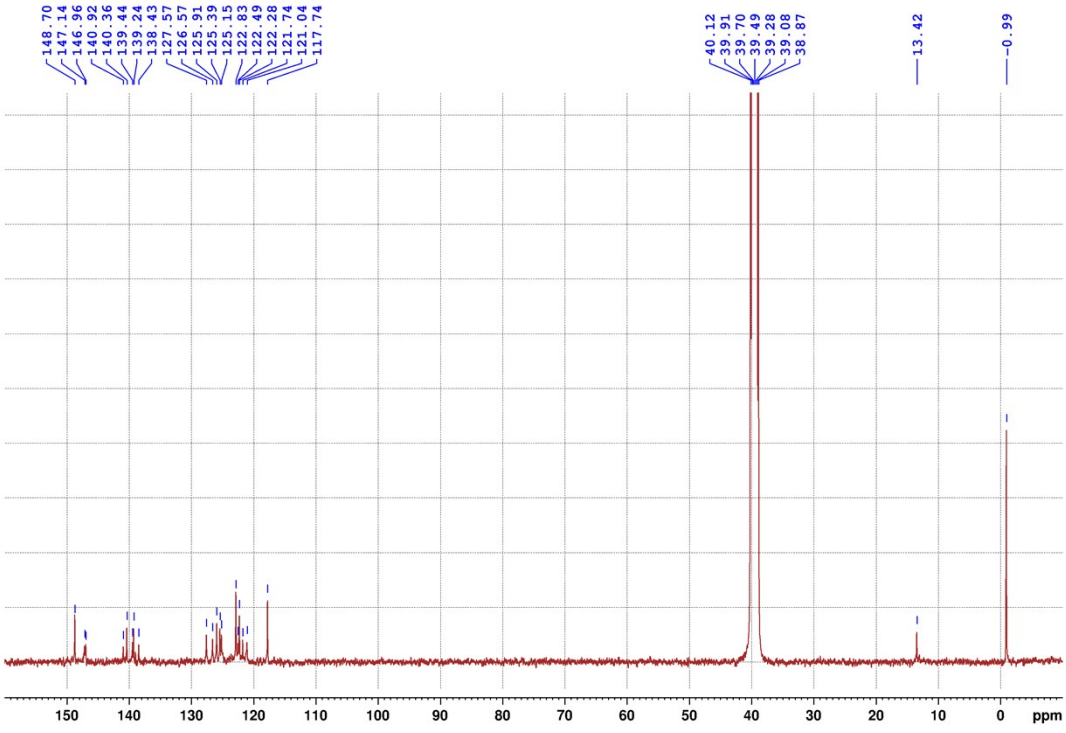

Figure S20. ^{13}C NMR spectrum of **2** in DMSO-d_6.

ESI mass spectra of complexes 1 and 2

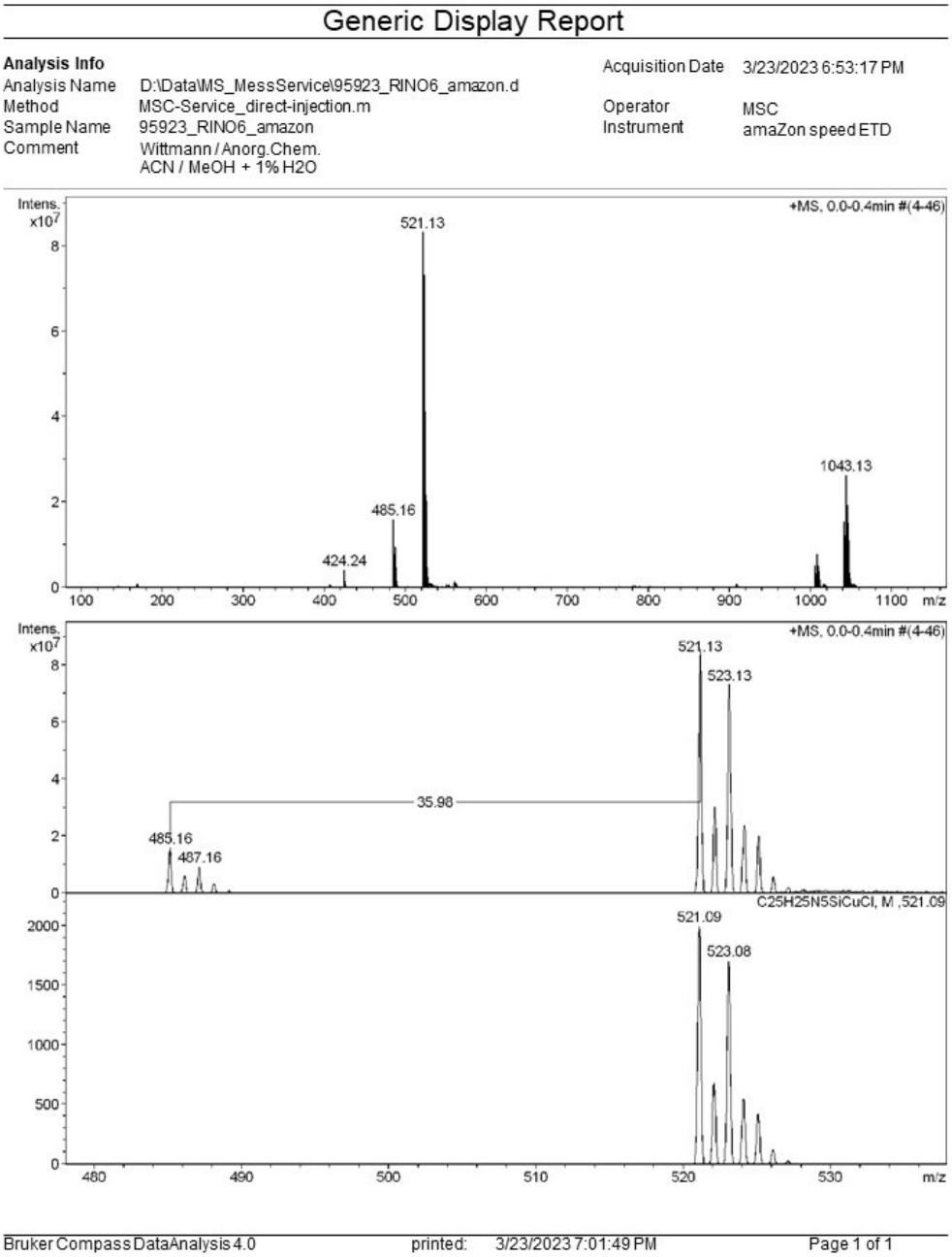

Figure S21. ESI(+) mass spectrum of **1**.

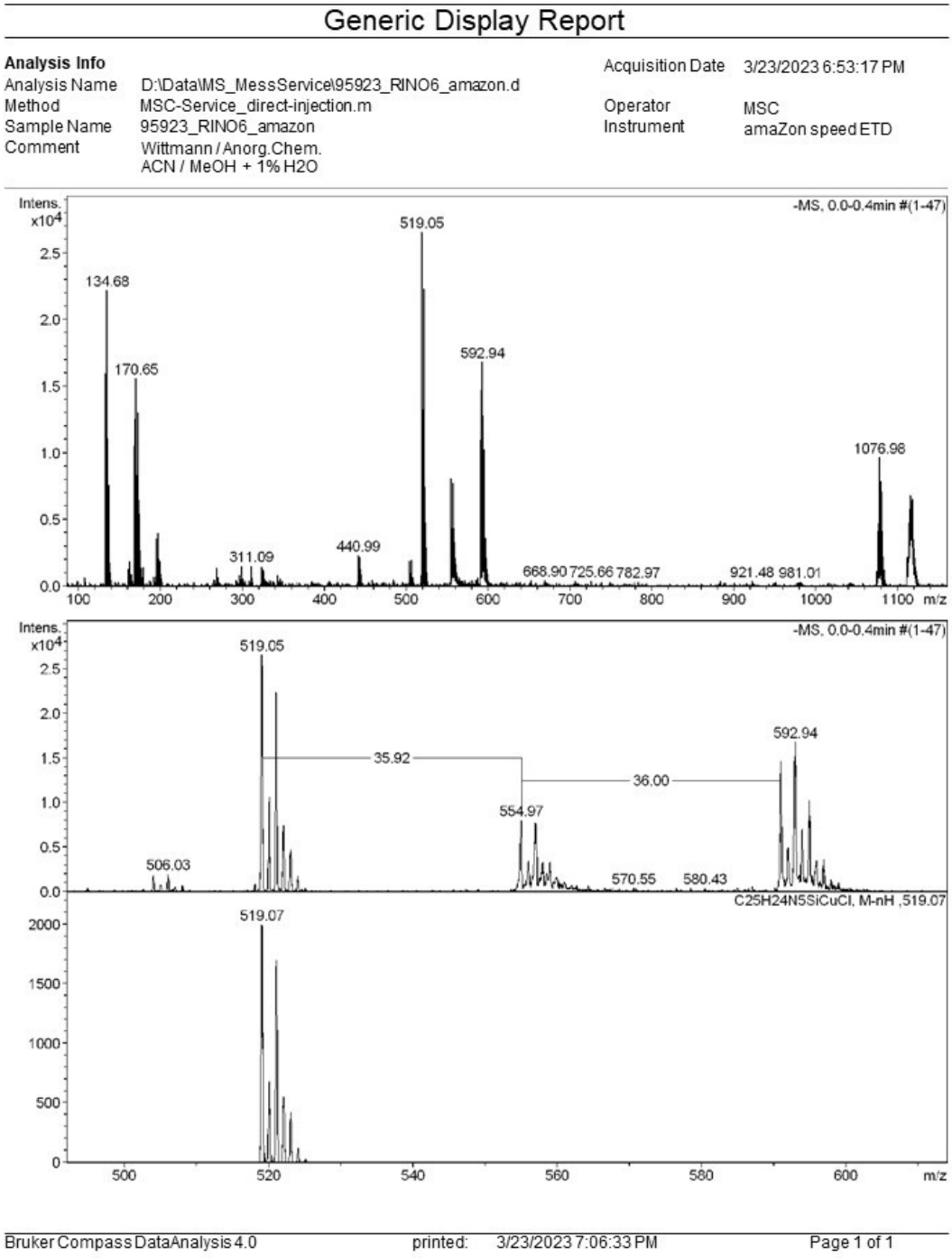

Figure S22. ESI(−) mass spectrum of **1**.

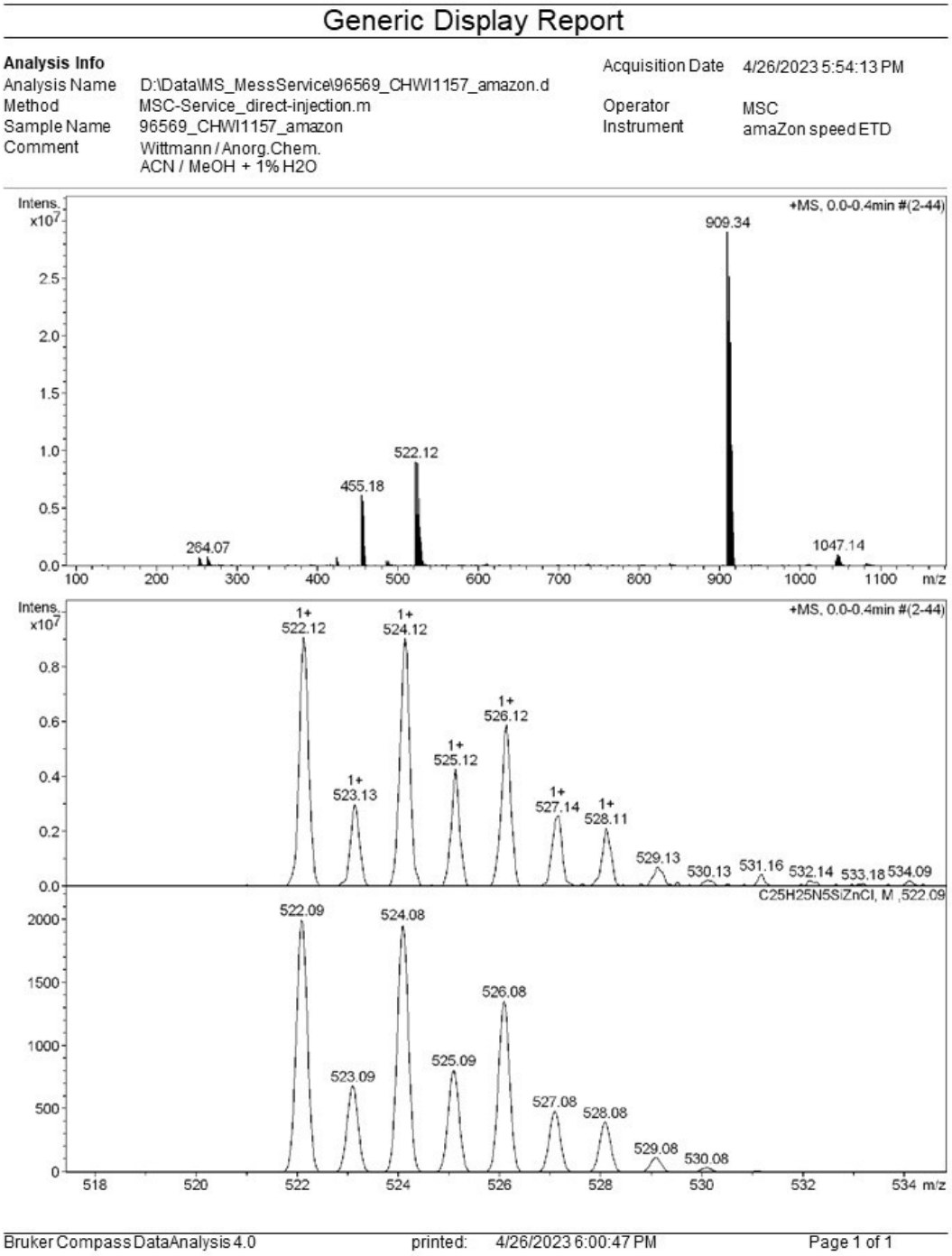

Figure S23. ESI(+) mass spectrum of **2**.

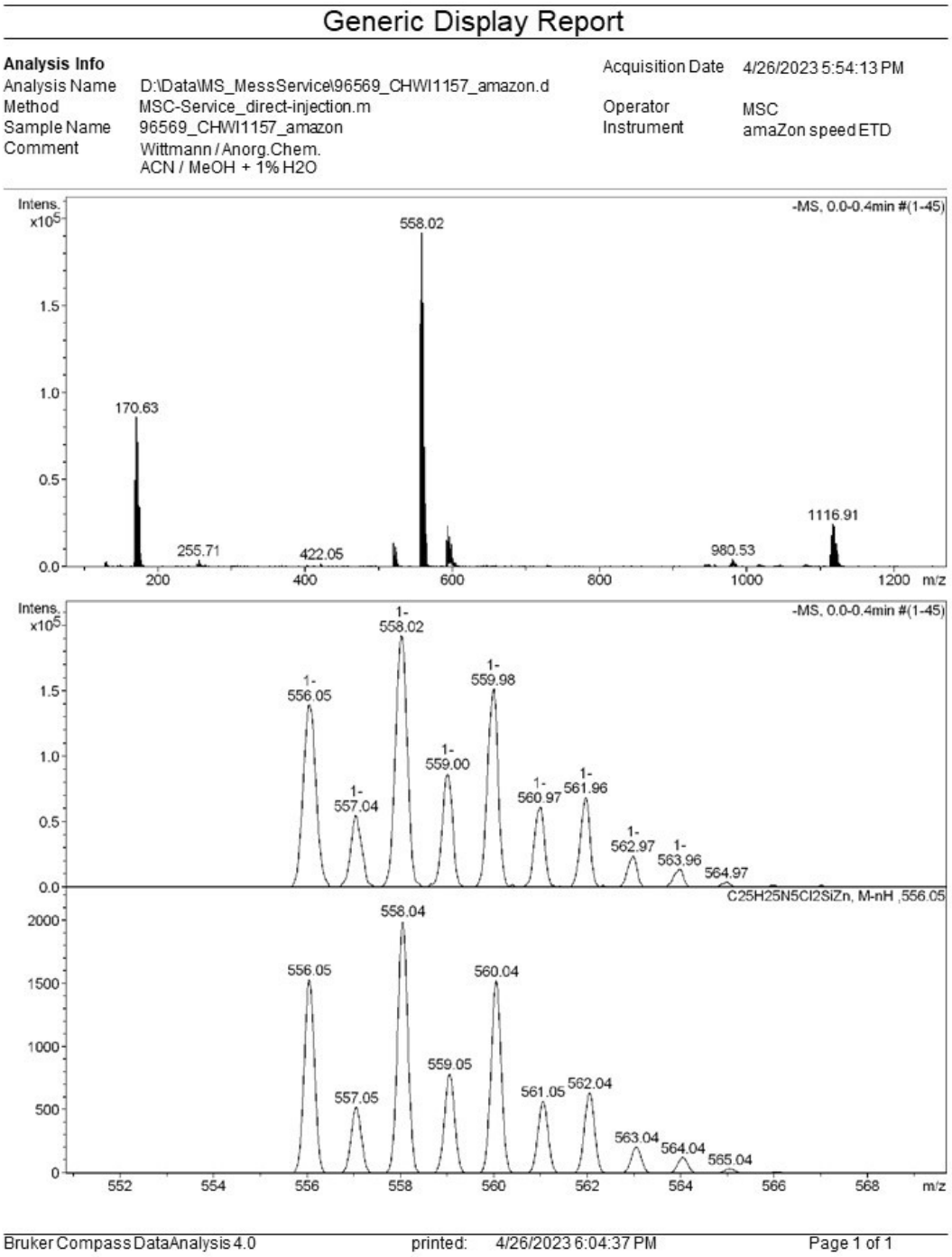

Figure S24. ESI(−) mass spectrum of **2**.

Crystallographic data

Table S1. Crystallographic data and refinement details for complexes studied.

Compound	**1**	**2**
empirical formula	$C_{25}H_{25}Cl_2CuN_5Si$	$C_{25}H_{25}Cl_2N_5SiZn$
fw	558.03	559.86
space group	monoclinic, $P2_1/c$	triclinic, $P\bar{1}$
a, Å	13.1421(7)	7.2600(14)
b, Å	14.3009(7)	12.210(2)
c, Å	14.7259(9)	15.930(3)
α,°		72.75(3)
β, °	94.735(5)	81.99(3)
γ, °		85.37(3)
V [Å^3]	2758.2(3)	1334.3(5)
Z	4	2
λ [Å]	0.71073	0.02508
ρ_{calcd}, g cm^{-3}	1.344	1.393
cryst size, mm^3	0.10 × 0.07 × 0.02	0.005 × 0.0013 × 0.0005
T [K]	100(2)	294(2)
μ, mm^{-1}	1.051	
R_1[a]	0.0854	0.2068
wR_2[b]	0.2770	0.4689
GOF[c]	0.894	1.382
CCDC no.	2378782	2378723

[a] $R_1 = \Sigma||F_o| - |F_c||/\Sigma|F_o|$. [b] $wR_2 = \{\Sigma[w(F_o^2 - F_c^2)^2]/\Sigma[w(F_o^2)^2]\}^{1/2}$. [c] GOF = $\{\Sigma[w(F_o^2 - F_c^2)^2]/(n - p)\}^{1/2}$, where n is the number of reflections and p is the total number of parameters refined.

Stability in solution

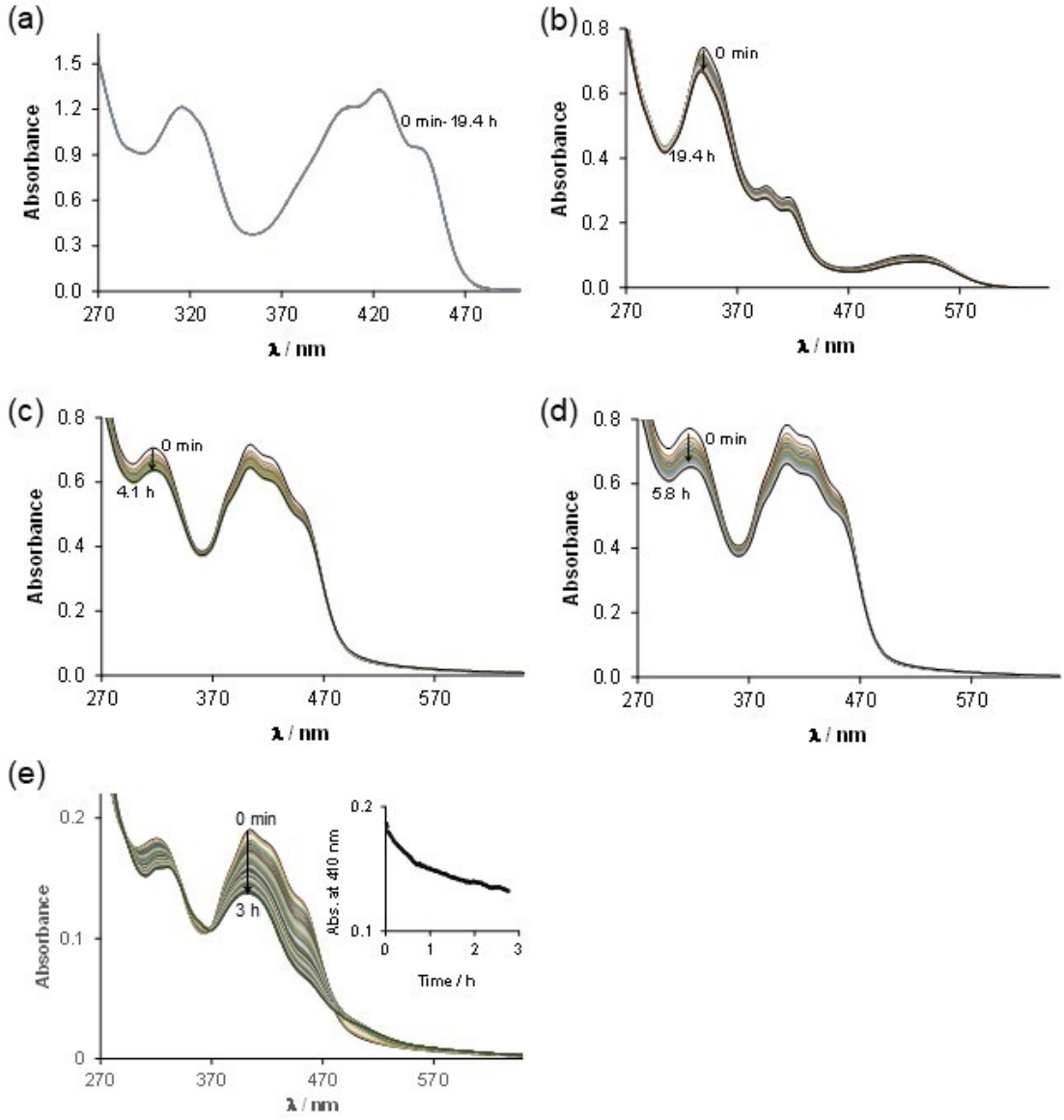

Figure S25. UV−vis absorption spectra recorded over time for **HL^{TMS}** in (a) DMSO, at pH (b) 2.0, (c) 7.4 (d) 11.7 and (e) at pH 7.4 under constant broad-band irradiation with a diode array photometer (D_2 + W lamp); {c = 50 μM (a-d) 12 μM (e); ℓ = 1 cm; T = 25.0 °C}.

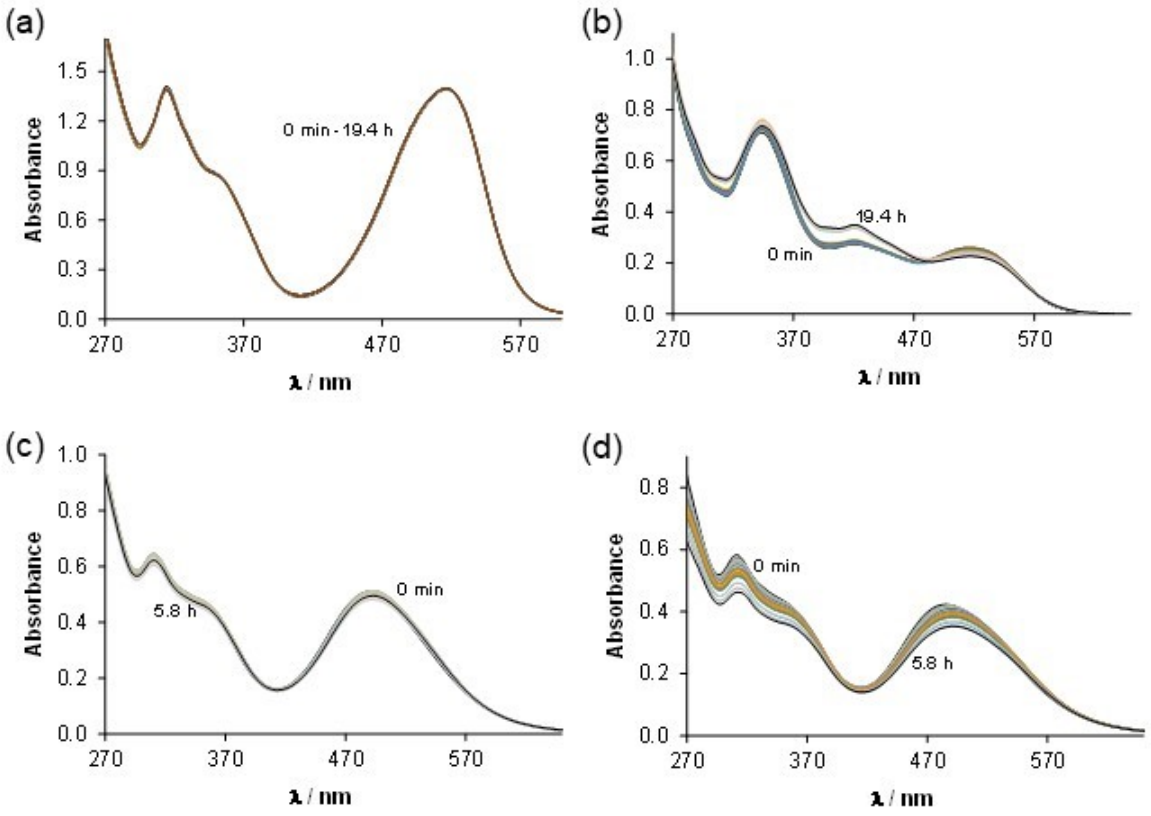

Figure S26. UV–vis absorption spectra recorded for **1** in a) DMSO, at pH b) 2.0, c) 7.4 and d) 11.7 over time; {$c = 50$ μM; $\ell = 1$ cm; $T = 25.0$ °C}.

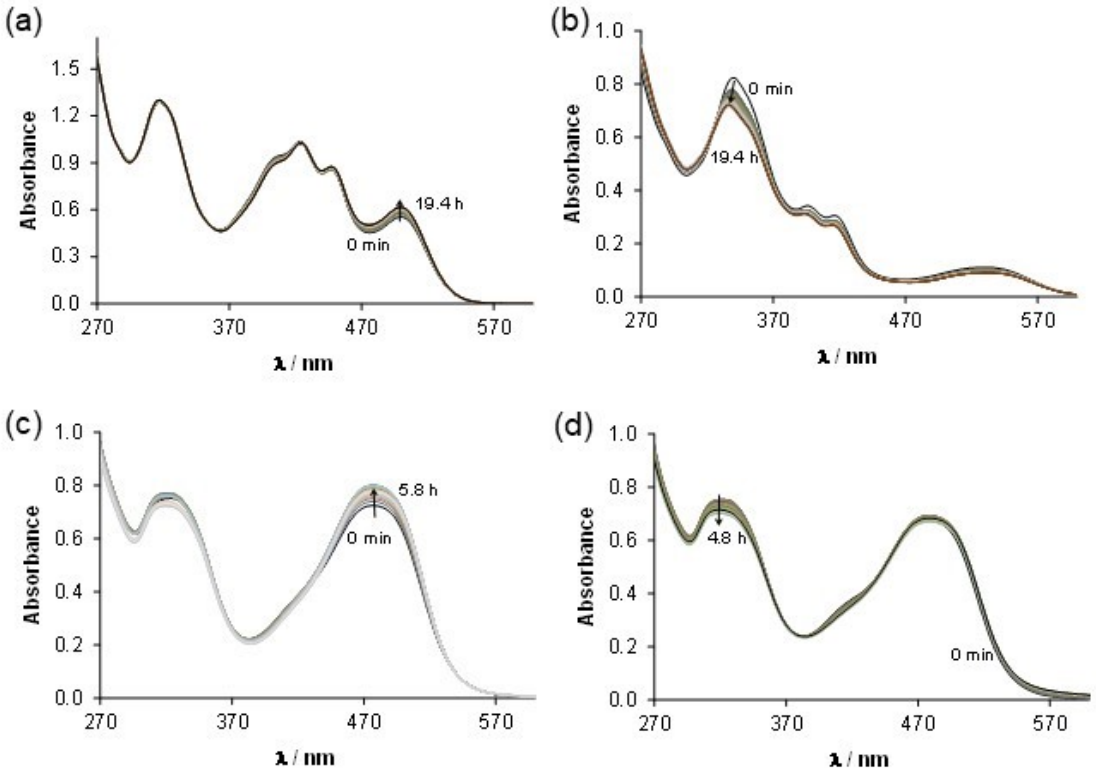

Figure S27. UV–vis absorption spectra recorded for **2** in (a) DMSO, at pH (b) 2.0, (c) 7.4 and (d) 11.7 over time; {c = 50 μM; ℓ = 1 cm; T = 25.0 °C}.

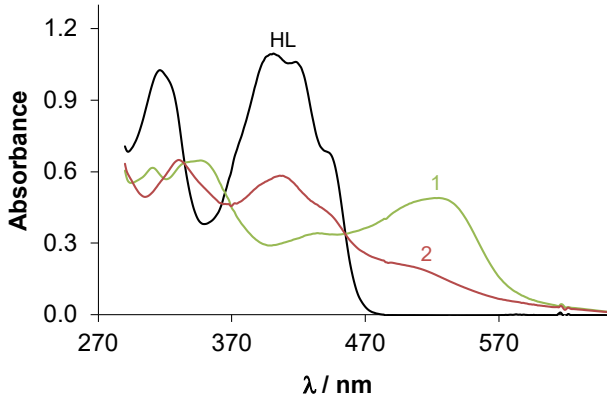

Figure S28. UV–vis absorption spectra recorded for the ligand **HL^{TMS}** and its complexes after dissolution in tetrahydrofuran; {c = 50 μM; ℓ = 1 cm; T = 25.0 °C}.

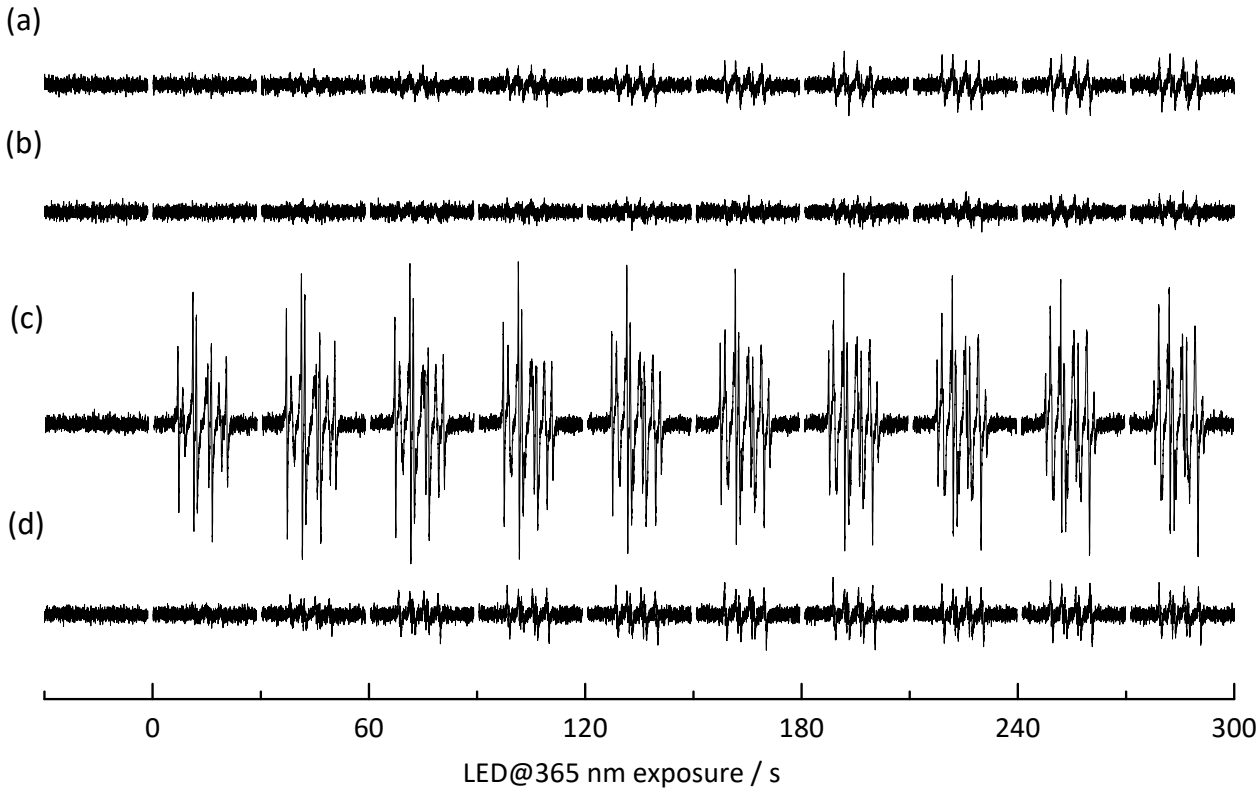

Figure S29. The time-courses of EPR spectra (SW = 10 mT) monitored upon LED@365 nm exposure (irradiance 18 mW cm^{-2}) of aerated (a) $\mathbf{HL^{TMS}}$, (b) **1**, (c) **2** in the DMSO and (d) **2** in the 50% (*v*/*v*) DMSO:H_2O solutions containing spin trap DMPO. Initial concentrations: *c*(sample) = 33 μM and *c*(DMPO) = 35 mM.

NCI-60 One-Dose Screening

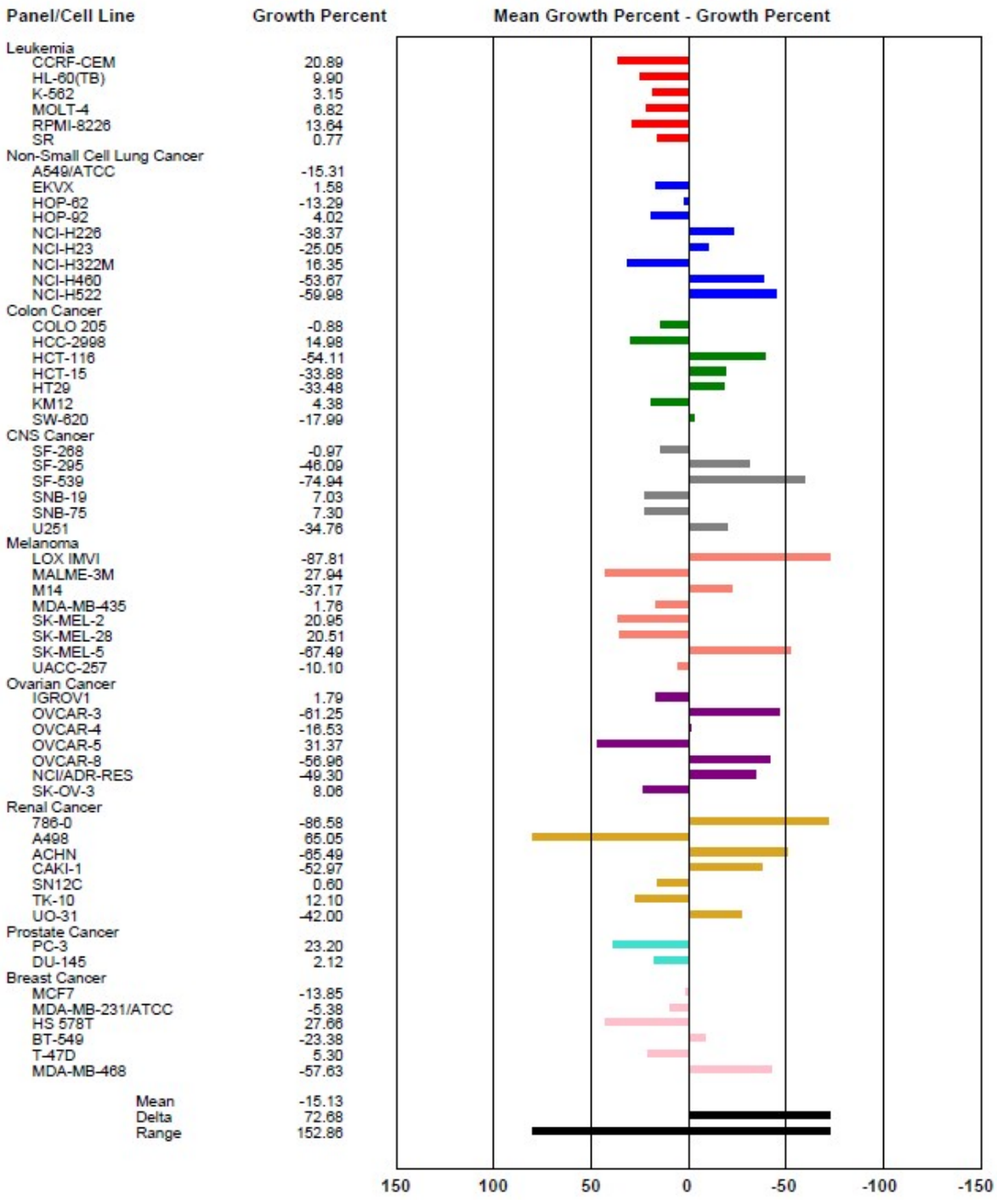

Figure S30. One-dose mean graph for **HL**^{TMS}.

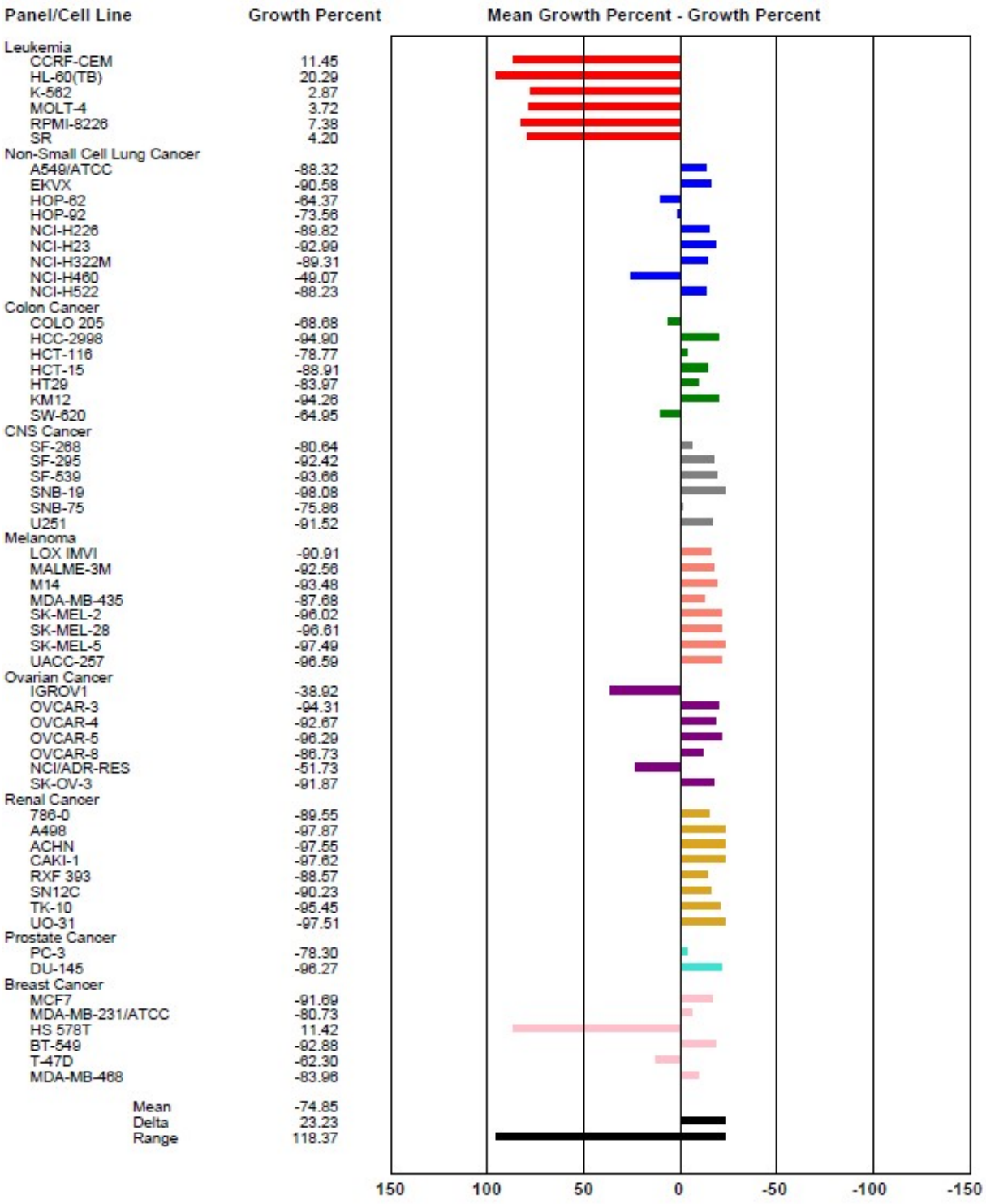

Figure S31. One-dose mean graph for **1.**

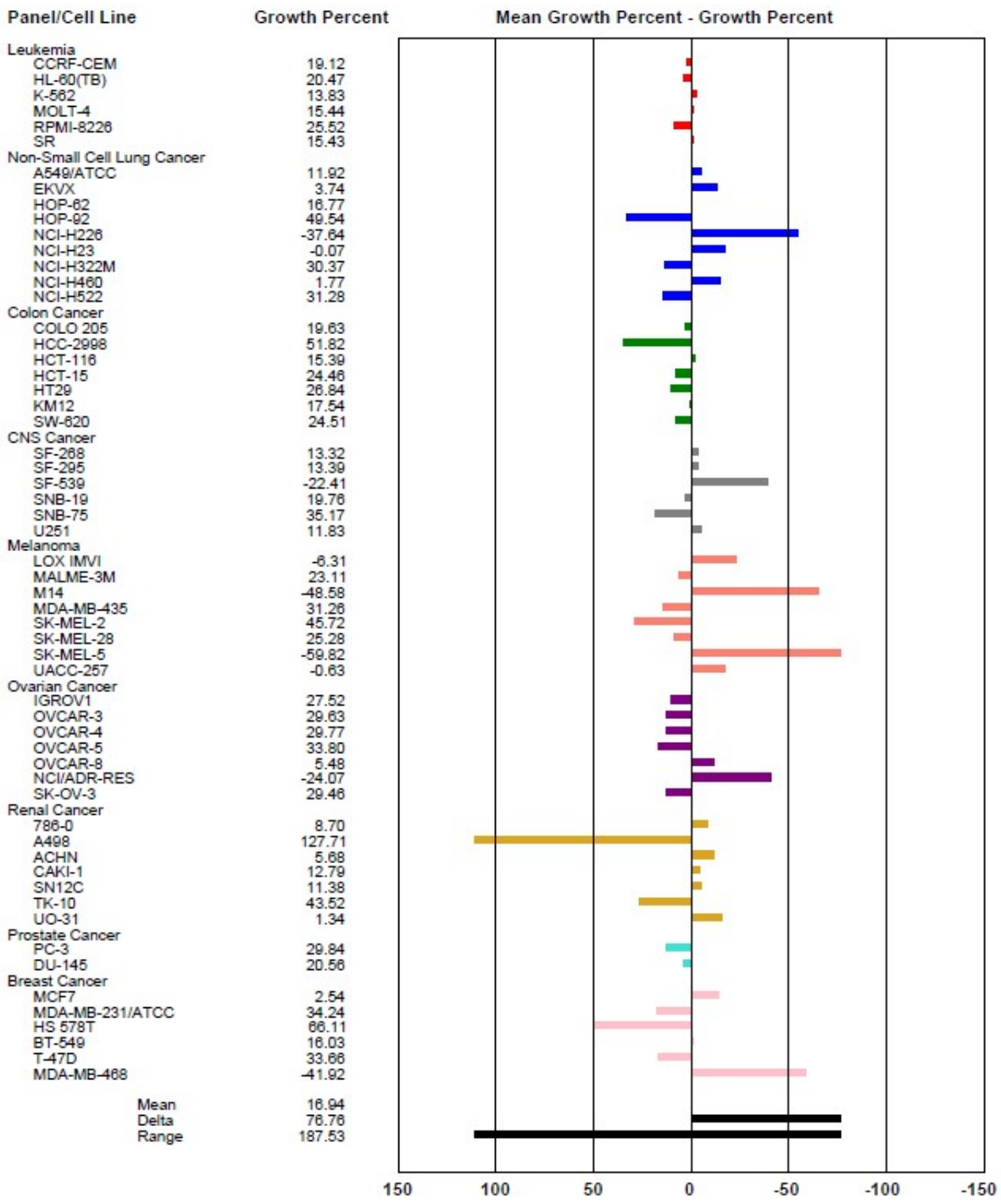

Figure S32. One-dose mean graph for **2**.

NCI-60 Five-Dose Screening

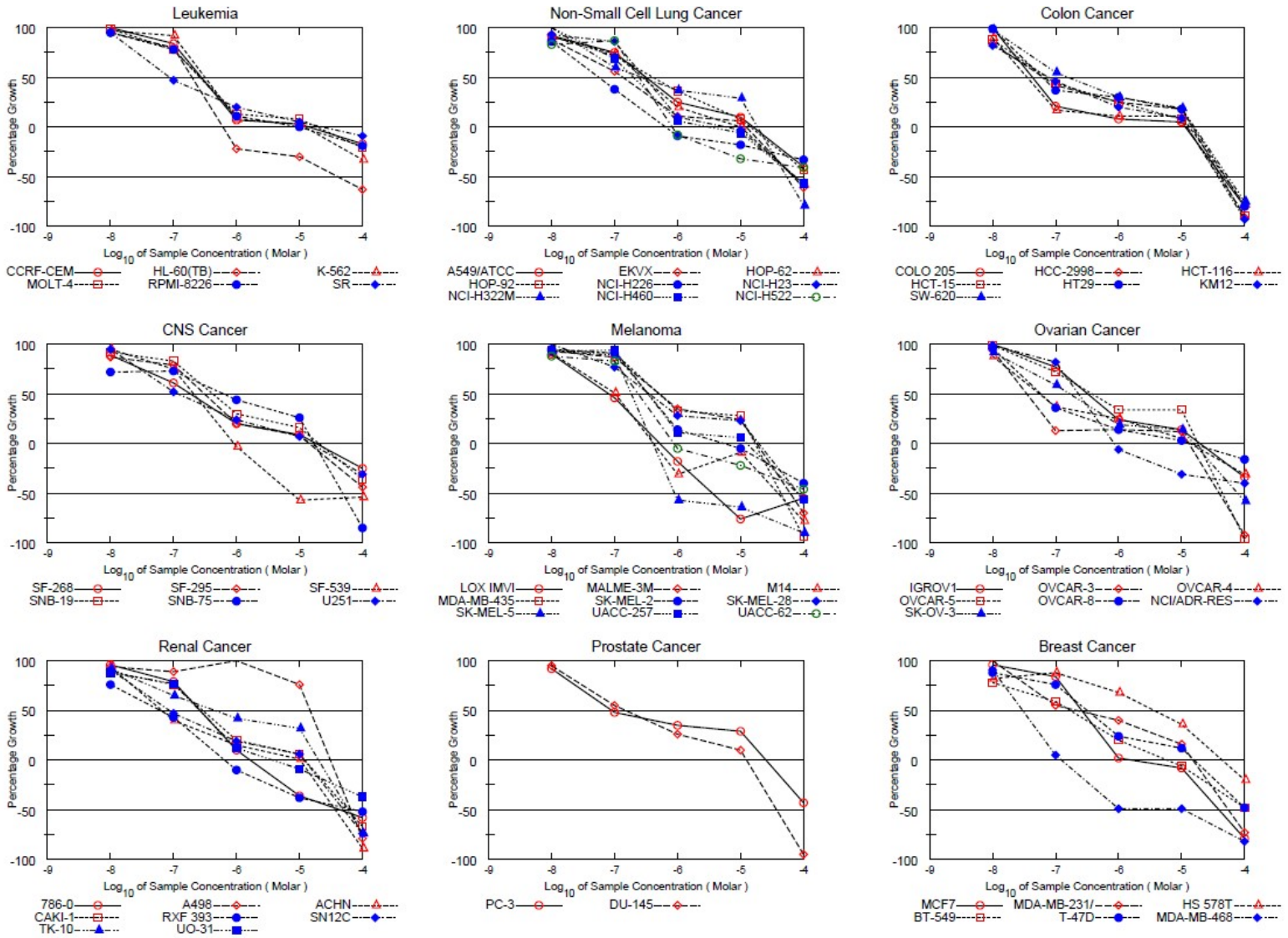

Figure S33. Dose response curves for **HL**^{TMS}.

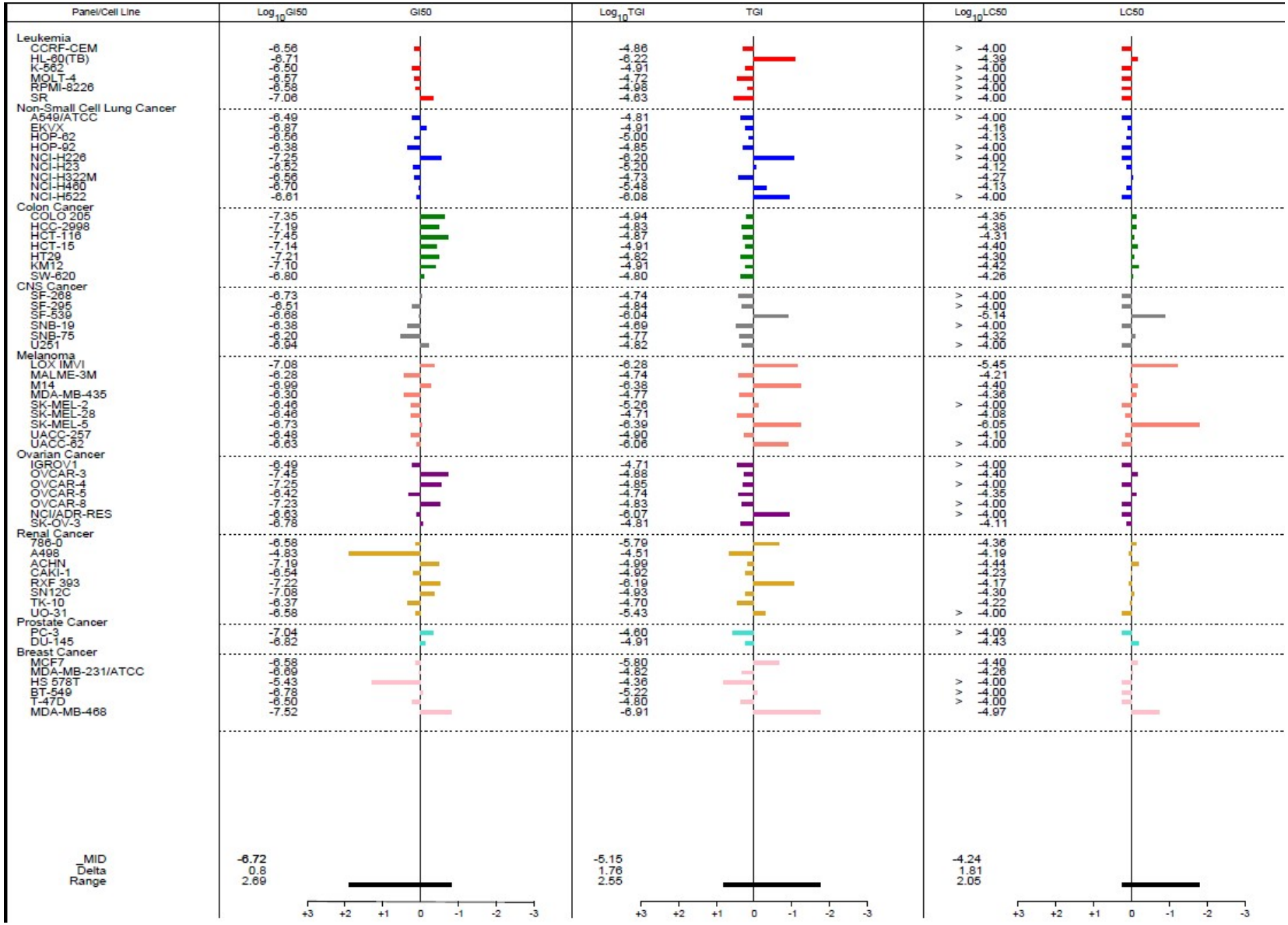

Figure S34. Five-dose mean graph for **HL**^{TMS}.

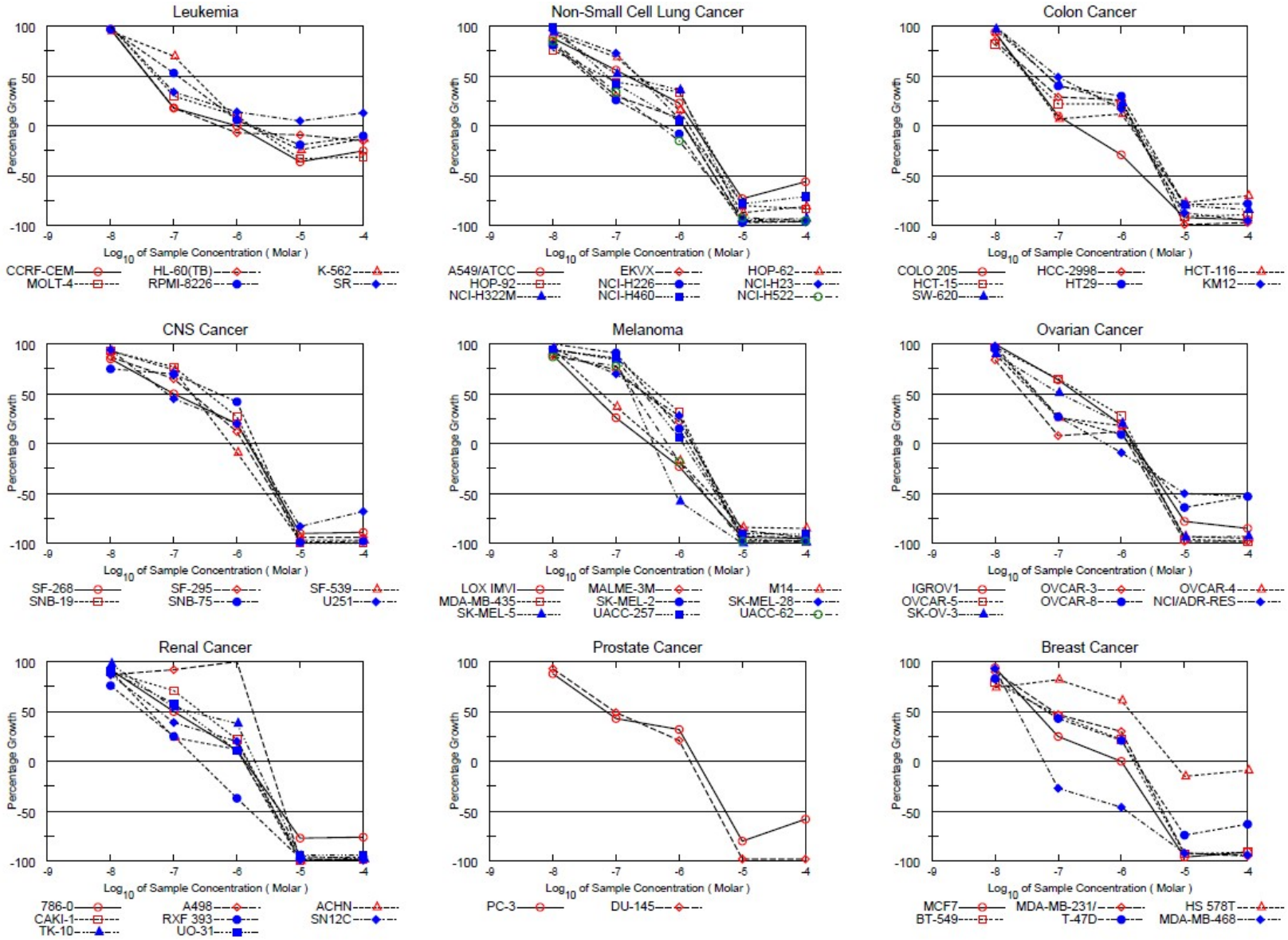

Figure S35. Dose response curves for **1**.

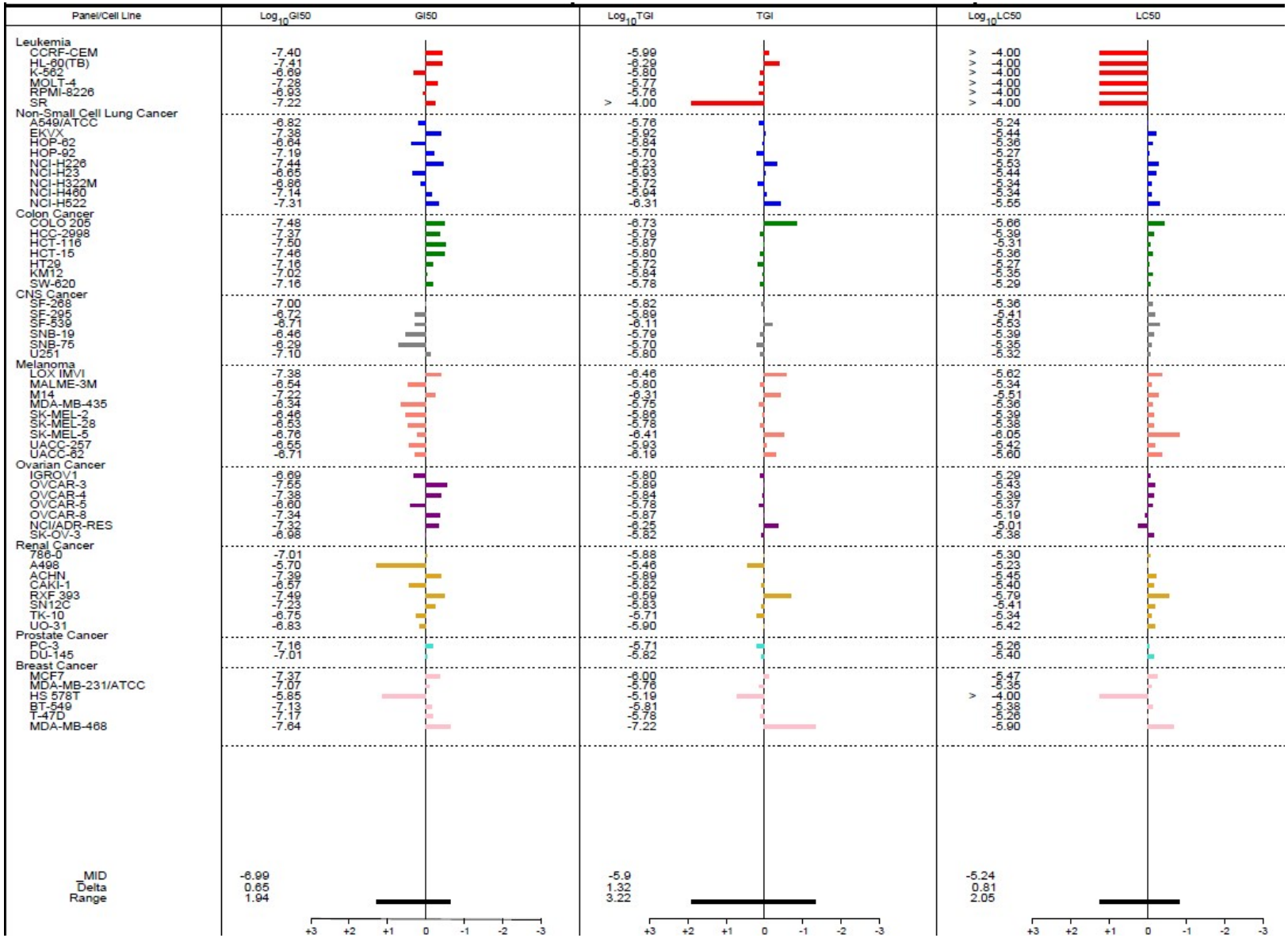

Figure S36. Five-dose mean graph for **1**.

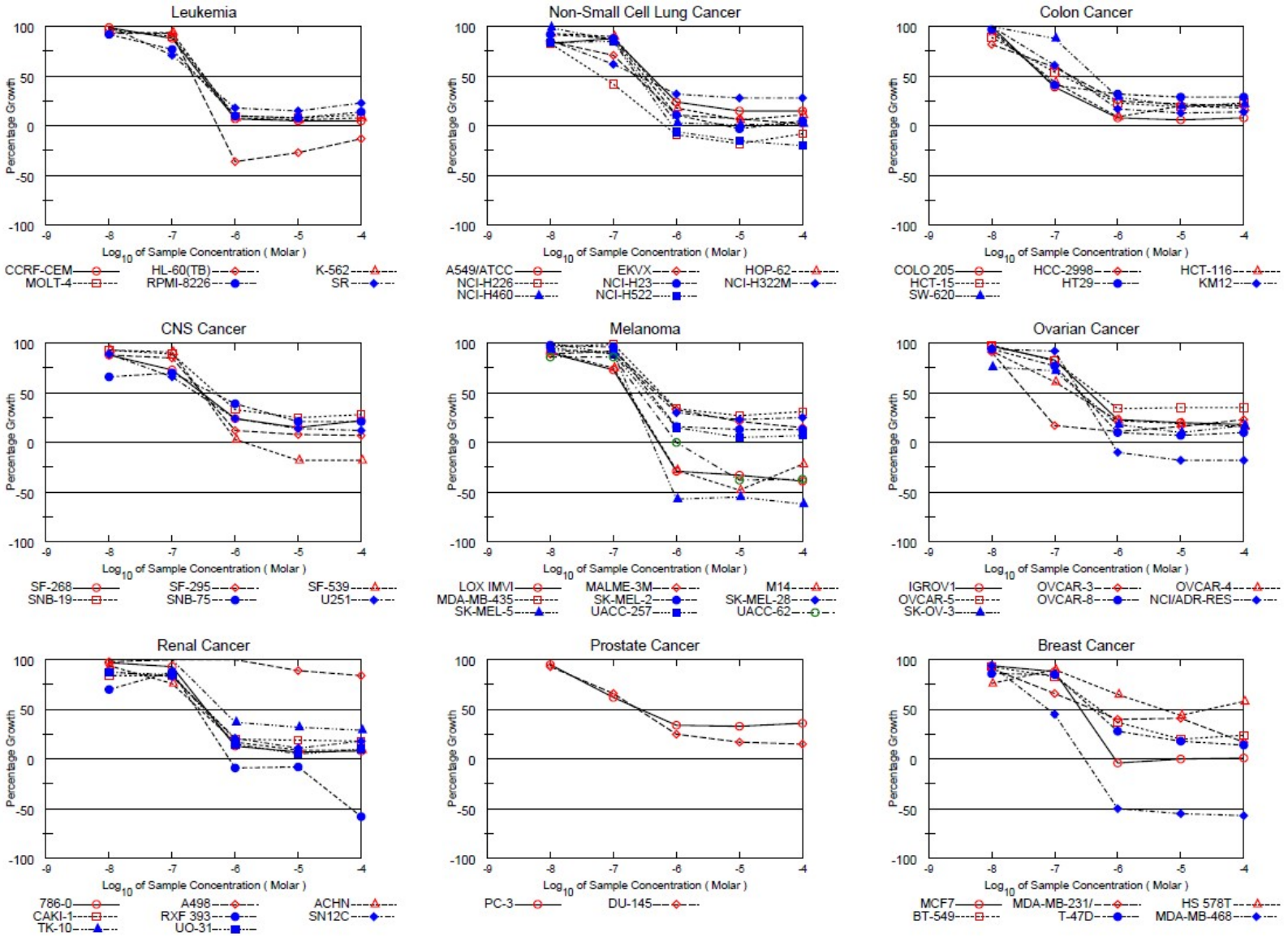

Figure S37. Dose response curves for **2**.

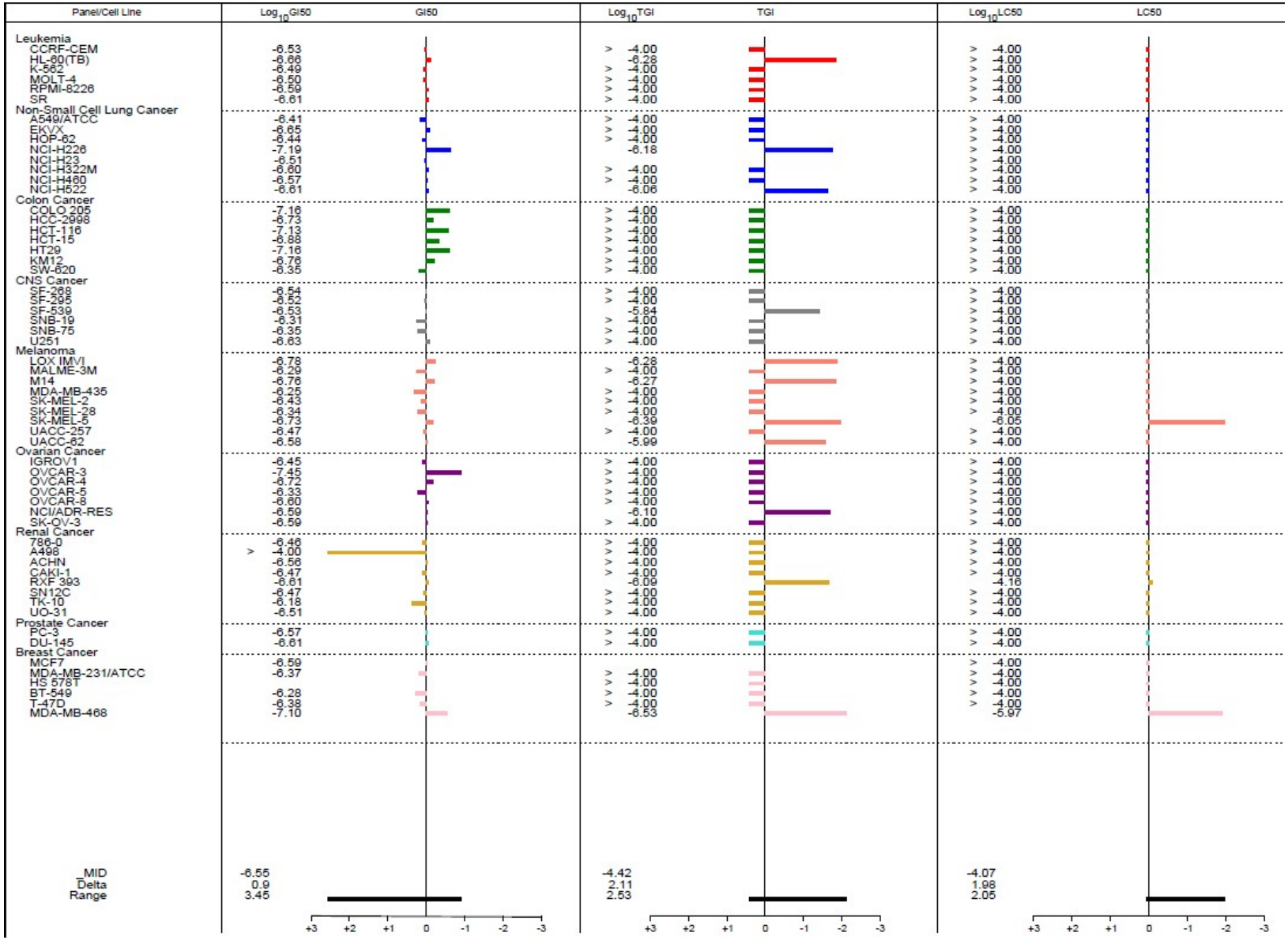

Figure S38. Five-dose mean graph for **2**.